PRELIMINARY DESIGN

Ground-based Remote Icing Detection System (GRIDS)

30 September 2001

NOAA Environmental Technology Laboratory
Radar Meteorology and Oceanography Division
Boulder, Colorado

Prepared for the Federal Aviation Administration, Aviation Weather Research Program
IN-FLIGHT ICING PDT (#4), TECHNICAL DIRECTION, FY2001
Task 01.4.3.3 Ground-based Remote Icing Detection System
FAA Icing Remote Sensing Testbed (GRIDS/FIRST)
Deliverable 01.4.3.1.E3

Table of Contents

Table of Contents (continued)

Executive Summary

In-flight icing annually causes high loss of life and property, and also a high cost for flight delays, cancellations, and re-routings caused by icing concerns that are perhaps needless. Therefore, the nation has a great need to improve its ability to forecast and observe in-flight icing conditions. In partnership with the Federal Aviation Administration (FAA), NOAA's Environmental Technology Laboratory (ETL) has for the past decade conducted research to develop a practical remote sensing system to help improve our ability to detect hazardous icing conditions aloft, and to provide accurate and timely assessment of local icing conditions. We call this system **Ground-based Remote Icing Detection System (GRIDS)**.

Our research has established that a radar measurement of the polarized scattering properties of clouds can be used to distinguish between two important categories of cloud particles – ice and liquid. It is liquid water particles that present an icing hazard, but they must be super-cooled and have sufficient water content to present a real hazard. GRIDS is designed for unattended operation. It will observe nearby clouds continuously, measure the amount of liquid water they contain, and determine if hazardous super-cooled spherical particles are present, *for every portion of the cloud from its base to an altitude of 10 km AGL*. To guarantee that even weak icing conditions high in clouds are detected, GRIDS must employ the most sensitive civilian cloud radar yet built. This is not a technical problem – the components are all commercially-available.

However, this high sensitivity radar is expensive and FAA funds are limited. We therefore discuss two versions of GRIDS – Target (fully-capable) and Upgradable (less sensitive). ETL will first build the Upgradable version by loaning the project expensive components at ETL's disposal (e.g., antenna, transmitter, radiometer). Target GRIDS will be better capable of assessing icing because of its enhanced sensitivity and more versatile pointing and processing capabilities.

GRIDS combines information from a "cloud" radar and a microwave radiometer, each developed by ETL, and by ingesting local temperature profiles from a reliable source (National Weather Service). GRIDS is a low-risk endeavor. It is an exercise in optimally configuring existing technology based on science, establishing a robust means for unified operation of the sensors, combining measurements with Web-based data automatically, and issuing real-time, easy-to-interpret assessments of icing hazard potential via the Internet. GRIDS will be housed in a transportable container. It requires only power, an Internet connection, and a clear field of view. A goal is to build Upgradable GRIDS in time to participate in the Aircraft Icing Research Alliance's (AIRA's) winter 2002-2003 campaign at Mirabel Airport, Canada.

1.0 Background

1.1 Introduction

Air traffic is increasing, spatial separations are decreasing, and aircraft in-flight icing is a growing threat to aviation, not only in the U.S. but worldwide. According to reports prepared for the FAA, aircraft accidents due to icing in the U.S. alone claim 30 lives annually, injure 14 others, and result in $96M in lost property (Paull and Hagy 1999). Icing conditions also disrupt air traffic operations resulting in large financial consequences for both airlines and passengers. Recommendations from a 1996 Federal Aviation Administration (FAA) workshop strongly emphasized the need to develop new remote sensors to detect Super-cooled Large Droplets (SLD) (Riley and Horn 1996; outlined by Reinking and Kropfli, 2000). [All references may be found in **References**, just before the Appendices.]

In-flight aircraft icing occurs when liquid cloud droplets or raindrops that are supercooled to temperatures below 0°C freeze on impacting the surfaces of an aircraft. Federal aviation regulations (Federal Aviation Regulation Part 25 Appendix C; FAR25-C) established two decades ago specify maximum tolerable icing conditions in terms of cloud liquid water content, cloud droplet size, and sub-zero temperatures (°C), but these guidelines consider only droplets less than 50 microns in diameter. Recent research has established that still larger droplets 50-500 microns in diameter can also present a severe hazard. These SLDs can penetrate the slip stream and freeze as rough ice on aircraft surfaces aft of the leading edge of the wing (Sand et al. 1984; Ashendon and Marwitz 1987; Politovich 1989; Cober, Isaac, and Strapp, 1995; Ashendon et al. 1996, Politovich 1996). Droplets both smaller and larger than SLDs tend to spread evenly on the airframe and therefore cause a less hazardous coat of ice than that typically made by SLDs.

However, all supercooled droplets above some minimum size present a potential icing threat. They are difficult to forecast and to detect. Currently-available operational weather surveillance systems are inadequate for use in detecting icing conditions, because of their wavelength, polarization, and scanning priorities.

This document presents the preliminary design of a prototype **Ground-based Remote Icing Detection System (GRIDS)**. GRIDS addresses the national need to help mitigate hazards caused by supercooled water in clouds. It is based on research sponsored by the Federal Aviation Administration (FAA) and conducted by NOAA's Environmental Technology Laboratory (ETL) over the preceding decade. Below, in Fig. 1, is a depiction of GRIDS supporting flight operations near an air terminal.

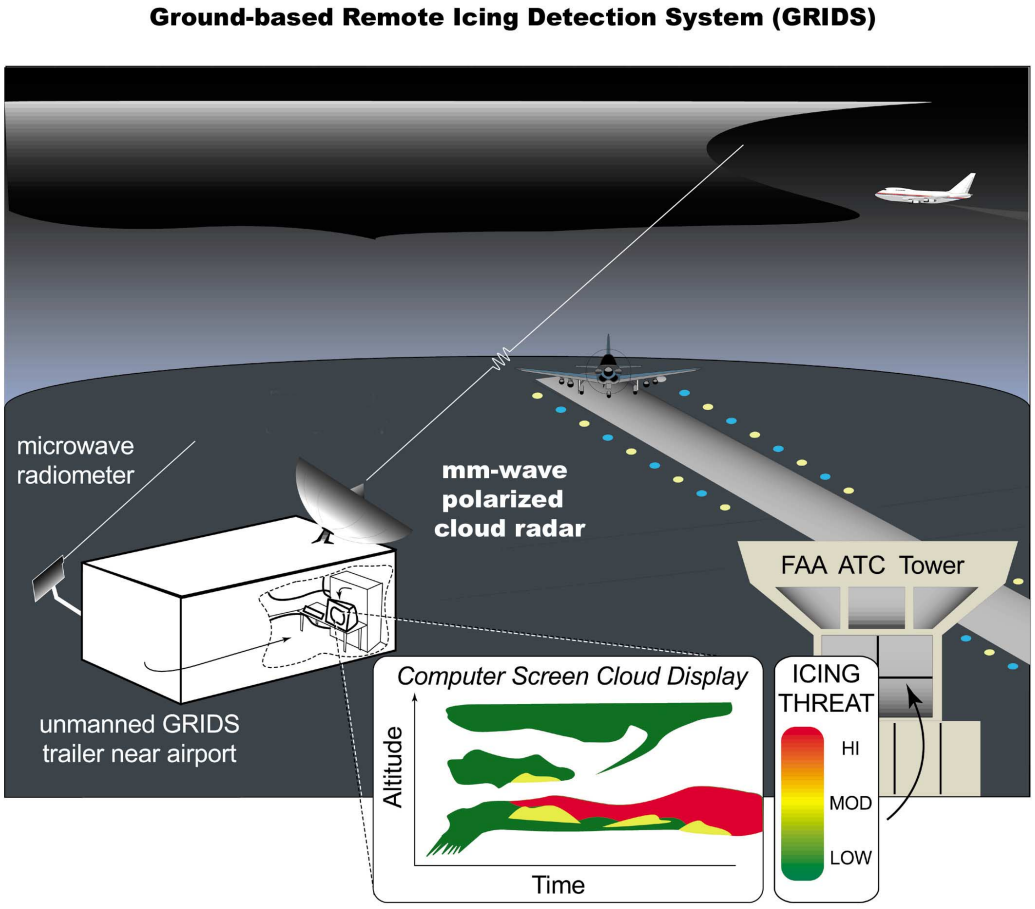

Fig. 1. Ground-based Remote Icing Detection System (GRIDS) near an air traffic center. GRIDS will operate continuously and unattended, providing automated warning of icing hazards within clouds, as depicted in the overlay.

In this Preliminary Design Review (PDR) document we discuss the many options that were considered in designing GRIDS, and the rationale for making specific choices. Product Development Team (PDT) management may direct ETL to change this preliminary design, or it may choose to endorse the design. This document serves as a resource and a reference for the FAA and for PDT management, whose job is to advance aviation safety and efficiency. It is also the plan by which the GRIDS team will build and demonstrate GRIDS.

1.2 History of Icing Hazards Research at ETL

Over the past decade NOAA ETL has, in partnership with FAA, investigated the use of both passive and active remote sensors to determine when icing condition exist aloft. We have used

theoretical modeling, instrument system development, and experimental observations. Each successive year sharpened the focus on observational methods that more confidently identify regions of hazardous cloud, and distinguish them from benign regions. A short history of ETL's research is outlined in **Appendix A**. It is also more thoroughly documented in ETL's final report for its PDT efforts in 2000 (available on request). The subject of this design document, the GRIDS prototype, is the culmination of this 10-year research effort.

2.0 Scientific Basis

2.1 Radar

The dual-polarization K_a-band cloud radar is the cornerstone of GRIDS. Its chosen operating frequency near 35 GHz is important because it is in an atmospheric "window" with little gaseous absorption to degrade signals. This frequency also allows the radar to easily detect small cloud particles, a much more difficult task for lower frequency radars (e.g., the NEXRAD radars used for weather surveillance). Another possible choice of frequency for GRIDS is near 90 GHz, the next higher "window" band. But at 90 GHz there remains significant (and time-varying) gaseous and liquid absorption, components are much more expensive, and transmitters are both less powerful and less reliable. At 35 GHz the size of the antenna is more manageable for the same angular beamwidth, and sidelobes are reduced with respect to weather surveillance radars. Reduced sidelobes have the advantage of eliminating ground clutter that can overwhelm the desired atmospheric signals at short ranges. At 35 GHz radar technology is relatively mature. This means that while components are more costly than at lower frequencies they are not exorbitant, and transmitter technology is robust and of sufficient power level.

As part of its decade-long icing hazards research, ETL tried but abandoned two-frequency (9.3 and 35 GHz) observations to detect super-cooled water in clouds, for both practical and scientific reasons. See **Appendix A** for explanations.

In its simplest design, the GRIDS radar will measure two parameters: equivalent radar reflectivity factor (Z_e) and depolarization ratio (DR), both at a beam elevation angle of about 40^o. DR is the primary measurement for GRIDS because it can be used to distinguish spherical from non-spherical particles. But Z_e is also important because it is related to the amount of water material per unit volume contained in the cloud being probed. In order to determine Z_e accurately, one must be assured of the radar calibration coefficients, which can drift and change. Hence it is important to routinely and automatically check the calibration of the GRIDS radar, which will be able to measure clouds with reflectivities down to approximately -59 dBZ at a range of 10 km. At this level of sensitivity (-29 dBZ in strong channel, -59 dBZ in weak channel), the GRIDS radar can measure DR accurately in a 10-km high cloud of mono-dispersed 20-micron droplets with a liquid water content as low as 0.06 g m^{-3}, or in a 400-micron droplet cloud with 10^{-5} g m^{-3} liquid water content, both well below the level of any icing hazard.

The radar will transmit purely polarized radiation and receive signals in two channels: one channel for the transmitted polarization (co-polar) and the other channel whose polarization is orthogonal to the transmitted polarization (cross-polar). DR is defined as a logarithmic ratio of

the radar reflectivity received in the weaker, cross-polar receiving channel to the reflectivity measured in the strong, co-polar receiving channel. Reflectivity factor Z_e is determined from signals in the strong channel. DR is determined by the shapes, orientation and density of the cloud particles from which the transmitted radar pulses are scattered. For particles whose geometric cross-section, as viewed by the radar, is nearly circular, very little depolarization occurs and DR is low. In fact, DR values from such circular targets are determined more by the imperfect properties of the receiving antenna and transmitter (i.e., polarization cross-talk) than by the scattering particles. Typical cross-talk values for linear and circular polarized signals are of an order -30 dB, for a radar like GRIDS.

Ice particles typically have non-circular geometric cross-sections, as seen by the radar, so they will produce depolarization ratios larger than the antenna cross-talk (except for some shapes like hexagonal plates, when viewed directly from below). Hence one can use DR and non-zenith view angles to distinguish non-hazardous ice particles from potentially-hazardous spherical water droplets (which provide circular geometrical cross-sections at any view angle).

Fig. 2 shows DR of different hydrometeors as a function of the radar elevation angle, as actually measured by ETL's scanning 35-GHz polarimetric Doppler radar during the recent Mt. Washington Winter Icing Sensors Project (MWISP) campaign in New Hampshire. There is a clear distinction between patterns of DR vs. radar elevation angle for drizzle (i.e., SLD if super-cooled) and these regular types of ice crystals. Irregular ice crystals (e.g., conglomerates) produce somewhat lower depolarization ratios (Reinking et al. 2001), but their DR values are still well above those for supercooled droplets at non-zenith elevation angles.

When the radar is pointed to the zenith (90^o elevation angle), planar-type crystals (e.g., hexagonal plates) produce DR values that are very close to that of water droplets (i.e., around -30 dB), because both types of particles have nearly circular geometrical cross-sections. However, at elevation angles well-removed from 90^o, there is a distinct separation between the DR values for spherical water droplets and any ice crystal, whose geometrical cross-section is now non-spherical. We choose for GRIDS an elevation angle near 40^o for several reasons. Higher elevation angles provide less differentiation in DR between spherical and non-spherical particles. Lower elevation angles will result in a significant increase of propagation path (i.e., the loss of sensitivity for upper layers) and introduce possible propagation effects (e.g., attenuation and phase rotation). Although it is not a primary function of GRIDS to study cloud ice, it should be mentioned that ice particle type (e.g., columnar vs. planar) and the evolution of the ice type is better established by measuring DR at two elevation angles (e.g., 90^o and 40^o). For such studies, Doppler velocity and velocity variance measurements at vertical incidence (90^o) can provide additional information (such as presence of significant updrafts and turbulence) that might improve detection of hazardous icing conditions, especially in mixed-phase clouds. Therefore, an optional capability for GRIDS is to transmit a vertical beam at 90^o elevation angle, in addition to its primary 40^o transmission.

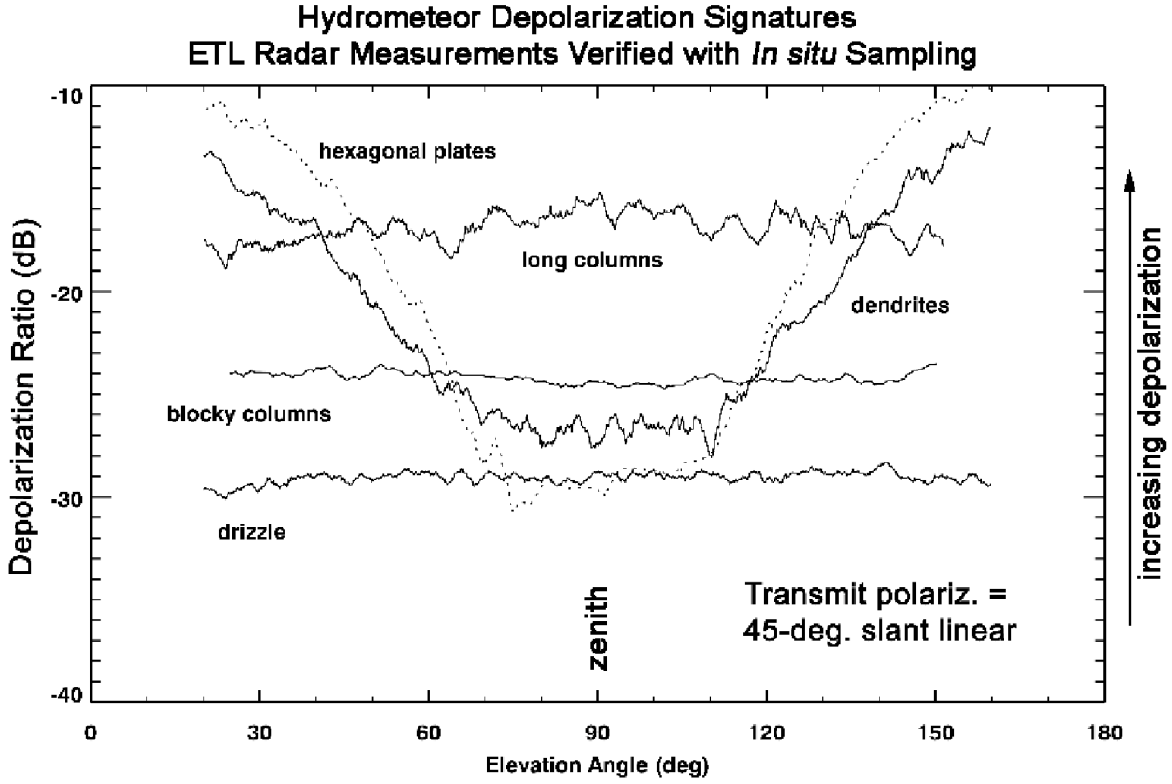

Fig. 2. Radar measurement of Depolarization Ratio (DR) vs. elevation angle for various *regularly-shaped* cloud particles during the 1999 MWISP campaign near Mt. Washington, New Hampshire.

The measurements in Fig. 2 were obtained by transmitting linear polarization at a slant angle of 45^{o}. This polarization is superior to standard horizontal polarization used in most weather radars (Reinking et al., 2002). Theoretical studies that incorporate real-life "flutter" effects of falling ice particles (Matrosov et al. 2001), show that a circular or near-circular polarization can provide even better separation in DR between ice particles and water drops. The introduction of slight ellipticity to the transmitted polarization will cause a stronger radar echo in the "weak" receiving channel. This will enable GRIDS to make meaningful measurements of even weaker reflectivity clouds. However, this ability comes with a price - transmitting elliptical polarization slightly diminishes DR separations between ice particles and water drops. For Target GRIDS we will specify the antenna and feed system to have circular polarization within standard limits of tolerance. However, it is almost certain that the delivered antenna and the transmitted state of polarization will be imperfect. We will measure the actual transmitted polarization state (i.e., its ellipticity) and the antenna's polarization cross-talk, and use those values to optimize the decision points in the icing algorithm. This same procedure will be followed for the borrowed

antenna for Upgradable GRIDS.

2.2 Radiometer

The dual-channel microwave radiometer has a well-proven capability for estimating total path-integrated liquid water (LW) amount and total path-integrated water vapor (WV) amount (Westwater 1972, Hogg et al. 1983). The technique is based on deriving the optical thickness of the atmosphere at two frequencies (e.g., near 24 and 31 GHz) by measuring the corresponding radiometric brightness temperatures and relating them to LW and WV. This is possible because at the selected frequencies optical thickness depends nearly linearly on LW, WV, and on the amount of oxygen in the atmosphere. The oxygen component is fairy stable and can therefore be accounted for with a high degree of accuracy. Selection of the two frequencies is important since the coefficients in the linear relations between optical thicknesses and LW and WV are frequency dependent and must be determined precisely. However, once the brightness temperatures are measured at the two frequencies, it is straight-forward to derive the path-integrated amounts of both water vapor (not of direct interest for GRIDS) and water liquid (of direct interest to GRIDS because this measurement helps determine the severity of icing hazard in super-cooled liquid water clouds).

3.0 Requirements

Based on what is scientifically feasible, ETL took it upon itself to write a requirements document for GRIDS. Normally this document is supplied by the sponsor, but FAA had neither the time nor the desire to generate it. ETL attempted to generate the requirements as a true proxy for FAA, and not let self-interest guide any requirement. However, the requirements do dictate certain aspects of the design. PDT management can review and alter the requirements. **Appendix B** contains the requirements document.

4.0 Preliminary Design

In the following sections we divide the overall GRIDS design into its major components and discuss each individually. Below in Fig. 3 is a simplified block diagram that shows how the various parts fit together and function. For a more comprehensive block diagram of GRIDS, see **Appendix C.**

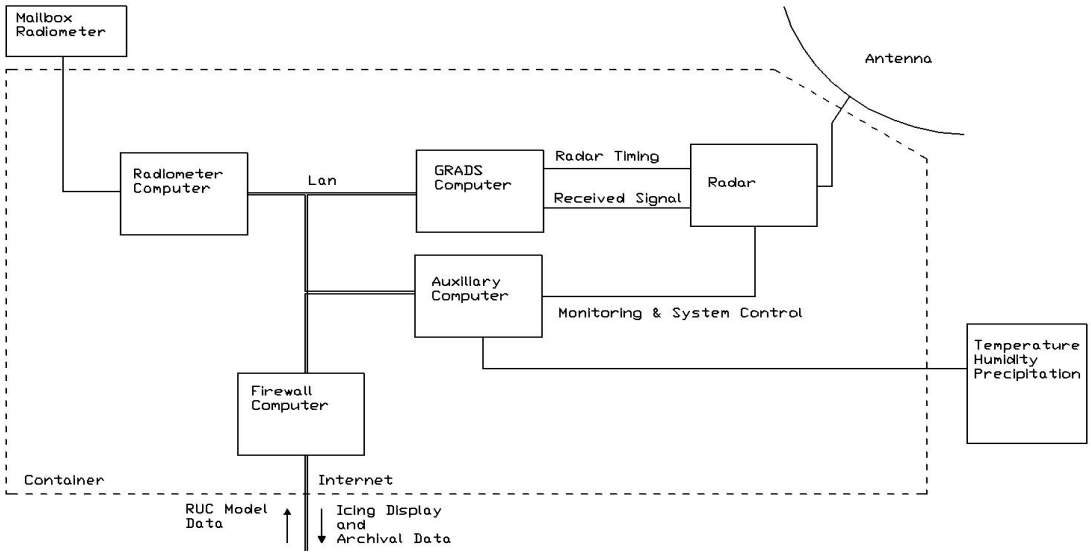

Fig. 3. Simplified block diagram of GRIDS showing all major sub-systems

"Target" GRIDS is the fully capable system. "Upgradable" GRIDS is the less than fully-capable interim system that will be built first with borrowed (less capable) components, in order to shorten the time to demonstration. As funds become available, the borrowed components will be replaced with permanent (more capable) components to achieve the target system. The table below summarizes the differences between the two versions of GRIDS.

Feature	**Upgradable GRIDS**	**Target GRIDS**
Transmit Power (Peak, w)	100	1000
Antenna Diameter (m)	1.8	3.0
Beam Pointing (elevation, º)	40.2	40.2, 90 (Option)
Radome	No	Yes
Icing Algorithm	Core	Refined
Autonomous Operation	No	Yes
Auto Calibration Check	No	Yes
Two Receiver Channels	No	Option
Spectral Processing	No	Option

4.1 Sensors

Research leading up to GRIDS indicates that the icing hazard within a cloud can be ascertained by combining three measurements – depolarization of microwave energy scattered from cloud particles, liquid water content along the path containing the scattering particles, and the

temperature profile within the cloud. These three measurements can be made using currently-available, proven technology. We discuss these technologies below.

4.1.1 Radar

The radar is the primary observing instrument for GRIDS, but it cannot alone make all necessary observations. It is based upon an award-winning design by ETL (Moran, et al., 1998) that has proven its power, flexibility, and robustness with more than 5 years of continuous operation at a number of remote Department of Energy (DOE) climate-observing field sites world-wide. It will be discussed here only in a cursory manner since its design is well-documented in the Moran paper. The final transmitter stage in DOE's Milli-Meter Cloud Radar (MMCR) systems, and in GRIDS, is a low peak power but high average power Traveling Wave Tube Amplifier (TWTA), designed originally for use in satellites. Average power is increased one of two ways (or both) with respect to more conventional final transmitter stages like magnetrons – high pulse repetition frequency (PRF) and/or transmitting pulses of long duration with embedded pulse coding (to maintain range resolution). For GRIDS, no pulse coding will be used to increase power (and hence sensitivity) because of complicating range-velocity sidelobes that can result.

Target GRIDS will have a TWTA with a peak transmitted power of 1000 watts. Upgradable GRIDS will be built first with a 100 w peak power transmitter, borrowed from spare NOAA components at ETL. Thus sensitivity for Upgradable GRIDS will be at least 10 dB less than design requirements, and likely even less sensitive because of the smaller borrowed antenna. TWTAs are designed to operate unattended for long periods of time, with the manufacturer stating an expected lifetime of 2.3 years. However, experience with DOE radars indicates that the actual lifetime of these devices is considerably longer.

All of the radar components are designed to function in a standard laboratory environment (76 degrees F, low relative humidity). The radar is therefore housed in two racks inside an environmentally-controlled transportable container, with the antenna mounted outside but as close as possible to the transmitter. The antenna will point the radar beam at a slant angle of about 40º above the horizon, or (optionally) straight up in the zenith direction (elevation angle of 90º).

The radar will have selectable pulse widths of 1.55 , 1.00, 0.6, and 0.3 microseconds giving range resolutions of 232, 150, 90, and 45 meters. We plan to use the 1.55 microsecond pulse width for the 40º pointing angle, and the 1.00 microsecond pulse width for the zenith pointing. Thus sensitivity at a given height above ground, and height resolution, will be approximately equal for the two pointing angles.

The desired minimum detectable signal at a height of 5 km above the radar is -130 dBm for target GRIDS, which corresponds to an equivalent radar reflectivity factor (Z_e) of -65 dBZ. [Henceforth we will refer to Z_e simply as reflectivity] Target GRIDS design allows the antenna elevation angle to be adjusted between 30º and 90º. Upgradable GRIDS will be able to adjust the antenna elevation angle only manually; most likely it will not be routinely adjusted, but kept fixed at 40º. Target GRIDS will have the capability for automatic angle changes commanded by

computer to one of two positions (most likely 40º and 90º), but this capability will not be implemented unless PDT management so instructs. For this capability, simple motors and stops would be added.

The microwave portion of the radar is shown in Fig. 4 in block diagram form. Here the single receiver channel is switched alternatively between two received polarization channels.

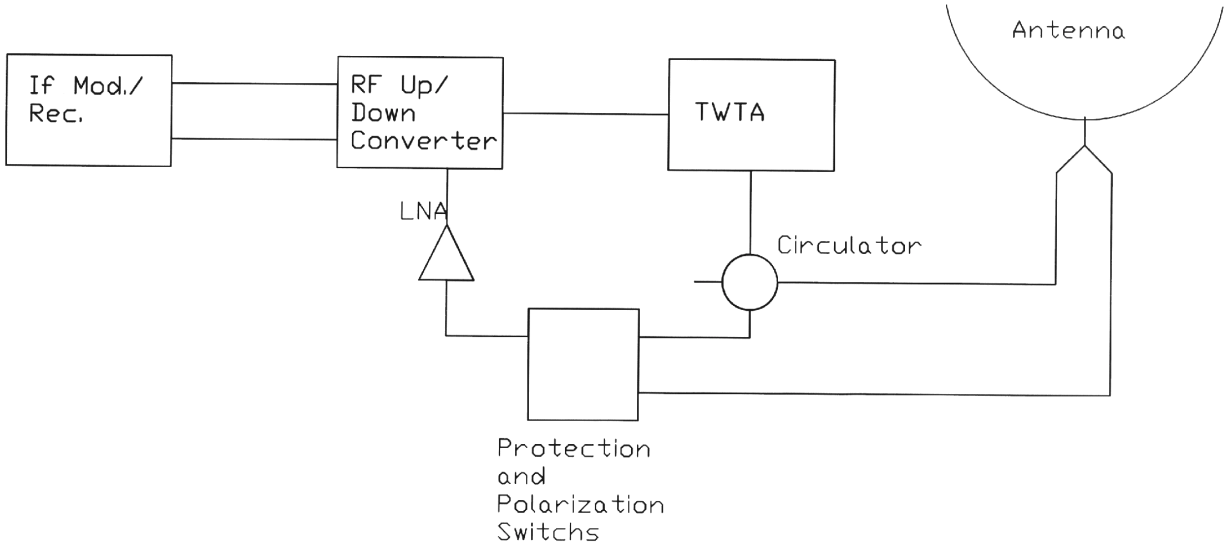

Fig. 4. Diagram of radar in GRIDS. One receiver channel is used for both polarization signals.

Calibration Checks: One planned difference between the GRIDS radar and DOEs MMCRs is the manner in which calibration checks will be performed. For MMCRs, about once every 10 days a lengthy process is undertaken whereby radar operations are halted and many different levels of white noise are injected into the receiving channel, a transfer curve is produced (signal in vs. detected power) for the entire dynamic range of the receiver, and the radar constant is re-derived and compared to the default value. All measurements are saved. Only if the new radar constant differs markedly from the default value is action taken. For GRIDS we will perform calibration checks much more frequently, at least once per day. Instead of regenerating the entire transfer curve, we will check only two points on it - one point near the center of the receiver dynamic range and one point at the bottom (no signal in). Action will be taken only if the transfer values differ markedly from the current "correct" values. Several years' experience with five MMCRs has led us to take this simpler approach. The more thorough and time-consuming procedure has no additional practical benefit. This procedure checks only the receiver's calibration; it does not check calibration of components "outside" the receiver, such as the waveguide between the antenna and the radar's electronics, and the antenna itself. These components typically remain stable unless damaged. The other variable is the transmitted power, which will be monitored.
Radome: Upgradable GRIDS will not have a radome since the borrowed antenna is not

configured with one. Radomes are antenna covers designed to protect the antenna from water build-up (snow/slush), and from birds and dust/dirt which are often a problem in unattended operation. The radome introduces a small loss by attenuating the radar signal on both transmission and reception (about 1 dB, two-way). This loss is normally accounted for in the antenna calibration, but additional loss will occur if the radome surface is coated with water or wet snow, perhaps during and after local events of precipitation. The amount of loss depends on the amount and thickness of water on the surface. For a vertically-pointing antenna the radome surface is nearly horizontal. Often such radomes are designed with a 5º tilt, to allow water to run off. Still, attenuation values range from a few dB to 10 dB, for radome surface wetness ranging from a thin film of water to puddles of water. For wet snow, several inches can add more than 20 dB of attenuation to the radar signal. The Upgradable GRIDS antenna, even without a radome, will still have some surface water film coating during and after precipitation that will attenuate the radar signals. Upgradable GRIDS will use a precipitation/wetness sensor to "flag" times when the antenna might be wet.

Target GRIDS' antenna must have a radome, to protect the surface of the dish from weather, birds, insects, etc. during unattended operations. Since the antenna will be tilted at an elevation angle of 40º either permanently or regularly, the likelihood of water/snow build up is reduced. The radome may, however, still have a water film build-up during and after precipitation that can introduce up to10 dB additional attenuation (two-way). The sensitivity of the radar will be reduced by this loss. The water film loss will not effect the depolarization ratio (DR) measurements since the loss is the same for both polarizations. The water film will effect the reflectivity measurement (calculated reflectivity will be lowered by the amount of the loss).

Receiver Channels: An option for Target GRIDS is to use two independent receiver channels, each dedicated to one of the polarization states. Digital Signal Processor (DSP) integrated circuitry would handle the increased raw data rate; the processed data rate after DSPs would be unaffected. This option would increase sensitivity of each polarization channel by 3 dB, equivalent to doubling the transmitter power. But it is considered cost prohibitive at this time, especially for Upgradable GRIDS.

4.1.2 Radiometer

The selected radiometer is a commercial unit with dual-frequencies, operating at 23.8 GHz and 31.4 GHz, built by Radiometerics, Inc. These two frequencies allow simultaneous determination of total liquid water and water vapor burdens along a selected path. The 23.8 GHz frequency was selected, in part, because it is in a reserved frequency band, free from satellite downlink transmissions that could contaminate any upward-pointed observation. ETL developed this technology originally in the late 1980s and helped transfer the technology to Radiometrics. Senior ETL staff (e.g., Dr. Westwater, originator of the technology) continue to support all radiometers of this type world-wide, including the one to be used for GRIDS. ETL has the experience and software necessary to take the commercial data stream and make it as accurate and reliable as possible in real time.

The radiometer head will be mounted on the roof of the GRIDS container, most likely on a corner that affords the best unobstructed field of view that is co-aligned with the radar bean. It will be capable of doing "tip cals" by swinging its 5-deg-wide beam through a vertical plane from horizon to horizon once per hour. Tip-cals work best under clear sky conditions. At all other times its beam will be co-aligned with GRIDS radar beam. The radiometer is operated by a PC inside the GRIDS container. The block diagram of the radiometer is shown below in Fig. 5.

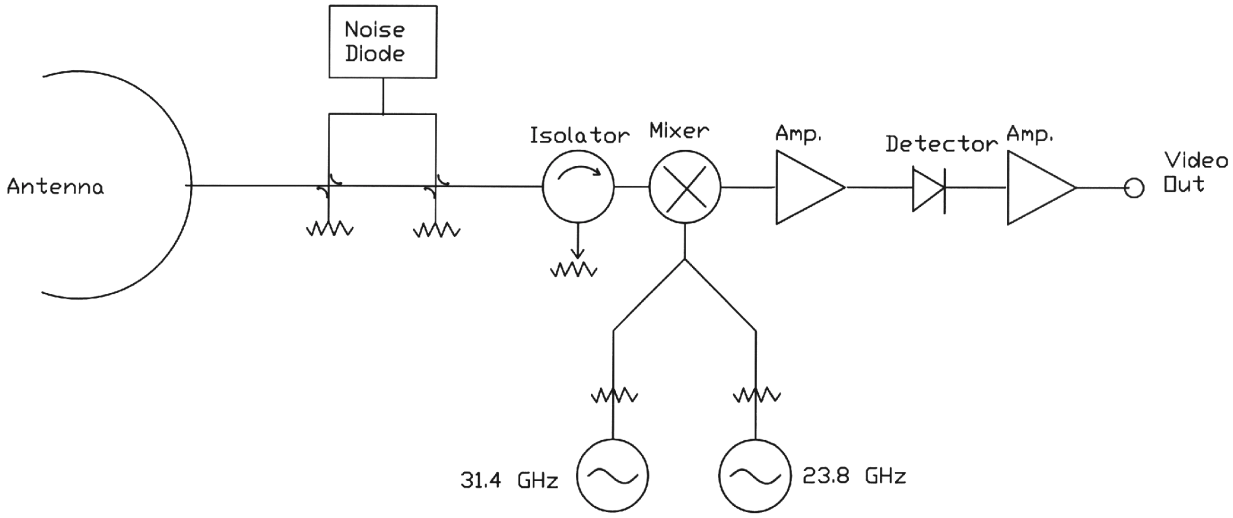

Fig. 5. Diagram of the 2-channel microwave radiometer to be used in GRIDS

This radiometer was chosen because it is commercially available, because it needs only slight modification to software for use in GRIDS, and because ETL has extensive experience in using it for research and in processing its data. Also, buying a commercial radiometer instead of building one at ETL saves money and provides long-term commercial support.

4.1.3 Temperature profiles

In addition to identifying the presence and altitudes of liquid water through radar and radiometer measurements, GRIDS must determine whether the detected liquid is supercooled. Timely information about the local vertical profile of temperature is therefore required. One approach is to measure the height of the "bright band" within clouds, the region of approximately 0 deg. C where falling ice particles melt and become water droplets, and where radar reflectivity is enhanced. Liquid water detected more than about 200 m above the reflectivity bright band is almost certainly supercooled. Unfortunately, bright bands are often difficult to detect or are not present at all, such as when the freezing level is at or just above ground level, or no precipitation is present. Thus, additional sources of local temperature information are required.

Two candidates for this information are nearby radiosondes flights and output data from numerical weather prediction (NWP) models; both are routinely and reliably available from NOAA Internet sites. Radiosonde launches typically occur only twice per day, they require 1-2 hours of flight time to profile the entire troposphere, and there may be 200-300 miles between launch sites. Thus radiosondes cannot be counted on to provide the timely and local information that GRIDS seeks, despite the fact that temperature fields aloft are less variable across large horizontal distances than surface temperatures, or cloud fields. Nevertheless, GRIDS design will allow ingest of closest radiosonde data and radiosonde temperature data will be available if needed.

GRIDS will depend most heavily on local temperature profile data obtained from a model. The Rapid Update Cycle (RUC) atmospheric prediction system, maintained by NOAA Forecast Systems Laboratory (FSL) and run at the National Center for Environmental Prediction (NCEP), produces updates with the highest frequency of any forecast and assimilation model in the United States. RUC is a combination of a data assimilation tool and a sophisticated mesoscale forecast model. Every hour, RUC issues updated meteorological analyses and forecasts. The analyses are based on data assimilated from multifarious sources including surface (land based and ship-borne), upper air (balloon-borne), and commercial aircraft flight-level (in situ) observations. The assimilation is performed via an optimal interpolation multivariate analysis procedure.

The analysis produces a self consistent statement of the current state of the atmosphere The current operational version, known as RUC-2, produces new three-dimensional analyses and forecasts every hour, covering the lower forty eight states at 40 km horizontal resolution and 40 vertical layers. A newer version of RUC is being tested with 20 km horizontal resolution, 50 vertical levels and with improved numerics in the assimilation package, as well as improved physics in the mesocale model. Real time access to RUC data is available from NCEP (http://ruc.fsl.noaa.gov/MAPS.rucinfo.html). These data will be ingested into the GRIDS/FIRST system via an Internet connection at hourly intervals.

4.2 Computer Operating System

As mentioned in section 4.1, the sensors to be used in GRIDS are to a large extent already developed. Much of the effort required to produce a reliable autonomous system like GRIDS lies in designing, developing, implementing, testing, and documenting the complex software that coordinates operation of the sensors, combines their disparate data streams, performs routine calibrations, gracefully handles every foreseeable contingency, and communicates with the outside world in a secure manner. ETL has extensive experience in all these areas.

Based on our experience with two different radar control and data systems (one for DOE cloud radars and one for ETL scanning research radars) we chose a VME-based system operating primarily under UNIX. With this choice we are able to embrace the latest generation of digital signal processor (DSP) technology, thus advancing capability and reducing DSP cost and risk for GRIDS.

Below we describe the design for the GRIDS system of computers, what they do, how they do it,

and how they interrelate. We believe this design will result in a robust unattended instrument at minimum cost and effort.

4.2.1 GRIDS Computer Architecture

GRIDS is designed with four computers, excluding the off-site archival system and Web server. See the complete system block diagram in **Appendix C** and the GRADS data flow diagram in **Appendix D**. Two of these computers are UltraSPARC systems built on a VME form factor; they perform the functions of radar control, data acquisition, and data fusion. The third computer is a PC that controls the radiometer; it takes data from the radiometer and calculates radiometer data products. The fourth computer, also a PC, functions as a network firewall. In theory several of these functions could be combined to possibly eliminate one or two of the computers. However, because of the low cost of PCs, the as yet undetermined workload for the UNIX machines, the simplicity of segregated functions, and the redundancy provided by multiple systems, it was decided to design GRIDS with four computers.

4.2.1.1 GRADS Computer

GRIDS Radar Acquisition and Display System (RADS) computer is the heart of the GRIDS data processing system. It is dubbed GRADS, as a combination of GRIDS and RADS. GRADS acquires, processes and displays radar data; ingests radiometer, surface meteorological and RUC model data; runs the icing algorithm; produces icing hazard displays; and exports data for archival and display. Physically, the computer is built in a 12-slot VME64x chassis, and contains the following VME boards: UltraSPARC CPU, DSP board incorporating four C6701 floating-point DSP chips, dual-channel 14-bit A/D board with buffer memory, a GPS board, and a Radar Timing Generator (RTG) board. All boards are Commercial-Off-The-Shelf (COTS) except for the RTG that is designed and built by ETL. RADS is described by Campbell and Gibson (1997).

The operating system used is Solaris 2.7, or later, which is an implementation of UNIX. The program which will perform the aforementioned functions is called the Icing Display and Data Acquisition System (IDDAS). This program is implemented in object-oriented C and C++, as a number of independent processes that communicate via shared memory.

4.2.1.2 Auxiliary Computer (AUX)

This computer performs the functions of monitoring and controlling equipment, and retrieving and pre-processing the RUC model. To simplify sparing in Target GRIDS, this computer is also built in a 12-slot VME64x chassis and contains the following VME boards: UltraSPARC CPU, 1-2 Industrial Pack (IP-pack) carrier boards that hold the A/D and digital I/O IP-packs. For additional detail on IP-packs see the Monitoring Section 4.4. The operating system is Solaris 2.7, or later, and almost all programs are implemented in LabVIEW. For Upgradable GRIDS, AUX will use a standard VME chassis and a SPARC computer.

4.2.1.3 Radiometer Computer

This computer sends commands to the radiometer to control its operation, receives the raw radiometer data via a serial line, and calculates both integrated liquid water and integrated water vapor. This time-stamped information is sent to the GRADS computer via a TCP socket every minute. The computer is a PC with passive backplane architecture, built in an industrial rack-mount chassis. The operating system is Windows NT 4.0, or equivalent, and the code is written in Microsoft C++. This computer can also archive the radiometer data to a zip disk if needed.

4.2.1.4 Firewall Computer

This computer acts as a gateway to the Internet for the other GRIDS computers. It centralizes security problems and provides system security for the other computers, protecting them from "hackers." This computer is also a PC with a passive backplane architecture, built in an industrial rack-mount chassis, the same as the Radiometer Computer. Its operating system is Linux.

4.2.2 Radar Data Acquisition and Processing

4.2.2.1 Data Acquisition

The radar is a dual-polarization, pulsed-Doppler radar with a high duty cycle. Although the transmitted polarization doesn't change, the received polarization is alternated every pulse. The radar receiver provides two channels of output, called in-phase (I) and quadrature (Q). I and Q feed a dual-channel A/D board which takes about 69 samples after each radar pulse. This results in a stream of data flowing in time order with alternating polarization after every radar pulse. This data is stored in buffer 1 on the A/D board. After a certain amount of data has been stored, the stream swings to buffer 2, and the data begins to be stored there. While this is occurring, the data is sent by a DMA transfer to the DSP board. When buffer 2 fills, the stream swings to buffer 1, and the process repeats. This swinging buffer arrangement allows the DSP ample time to react to the data stream.

4.2.2.2 Front-end (DSP) Processing

Data from the 14-bit A/D is staged in an area called global memory on the DSP board. The number of range gates is then divided (approximately) by four, and each of the four DSPs fetches from global memory the data associated with its assigned range gates. This scheme insures that the processing load is distributed evenly among the four DSP chips, and that "load-balancing" between the DSPs does not become an issue.

The DSPs perform the calculations described in the GRIDS Covariance Algorithms document (**Appendix E**). Note that there are two classes of results from these calculations: recorded data products and display products. Because the display products can be recalculated from the recorded data products, they will not be recorded. They are calculated solely for the purpose of

providing real-time displays and as input for the icing algorithm.

When the DSPs are done with their calculations, they write their results into contiguous areas of global memory. A small packet header is affixed to the beginning of each DSP-processed block of radar data; this packet contains information such as beam serial number, time (obtained from the GPS board), elevation angle and polarization. An interrupt is raised to notify the UltraSPARC that the data is available.

4.2.2.3 Back-end (SPARC) Processing

When the IDDAS, which is running on an UltraSPARC, receives the interrupt from the DSP, a process called readDMA transfers the data by a DMA operation. It then calculates and appends header information and sends the recorded data products through shared memory to another process, writeDisk, which writes these records to disk. At the same time the readDMA process sends the display data products to another process, xDisplay, which displays the radar data.

Simultaneously another IDDAS process ingests radiometer data via a TCP socket. Using shared memory, another process writes the radiometer data to disk while the updated radiometer data is displayed in real-time. Similarly there are processes which read and write surface met data and RUC data (sections 4.2.4 and 4.2.5 below). Another process calculates the icing hazard every minute throughout all portions of detected clouds and sends results for display.

For more details, see **Appendix F** (Software Capability Specifications for GRIDS IDDAS).

4.2.3 Radiometer Data Acquisition and Processing

The Radiometer Computer acquires data through a serial port, calculates liquid and vapor column amounts, and reformats the data. It then sends the data to the UltraSPARC via a TCP socket, where the data is ingested, written to disk and displayed in real-time by IDDAS.

4.2.4 RUC Model Data Processing

The AUX system will acquire RUC model data from the Web site and will reformat the data. It will then write time-stamped files on the UltraSPARC's disk via FTP. A separate IDDAS process on the UltraSPARC will read those files.

4.2.5 Surface Met Data Processing

The AUX system will acquire surface meteorological data from GRIDS sensors and send surface temperature and humidity data to IDDAS via a TCP socket. Separate IDDAS processes will read and write the data stream.

4.2.6 Icing Algorithm Processing

There will be an IDDAS process on the UltraSPARC which accesses the latest radar, radiometer,

surface meteorological and RUC data via shared memory and calculates the icing hazard potential. Once that calculation has been made, the numerical information needed to color-code icing hazard displays will be sent via shared memory to the radar display process, xDisplay. Here data will be displayed and communicated externally. The icing algorithm is discussed more thoroughly in section 4.3.

4.2.7 IDDAS User Interface

The IDDAS user interface, RCP, runs on the UltraSPARC. It communicates with the rest of the GRADS processes via shared memory. RCP communicates with the AUX and Radiometer Computer via TCP sockets. An operator can view, build, modify, check, save, load, and run control tables and queues of control tables. It allows the operator to start, stop and position the radar and radiometer, to tell the AUX machine to stop sending RUC and surface data, and to turn on and off data archival. Status messages and a help menu will be available via the user interface. See the GUI prototype in **Appendix F**.

However, for autonomous operation no operator will routinely exercise the user interface. Instead, the user interface will be available for intervention (if needed) and to display health and status information to personnel visiting the container.

4.3 Icing Hazard Algorithm

.

The core icing algorithm uses four decision points based on the slant-path, fixed beam measurements of liquid water (LW), radar reflectivity Z_e, radar depolarization ratio (DR), and on the ingested temperature profile. Fig. 6 depicts the decision tree used to determine icing potential as a function of altitude (H_i).

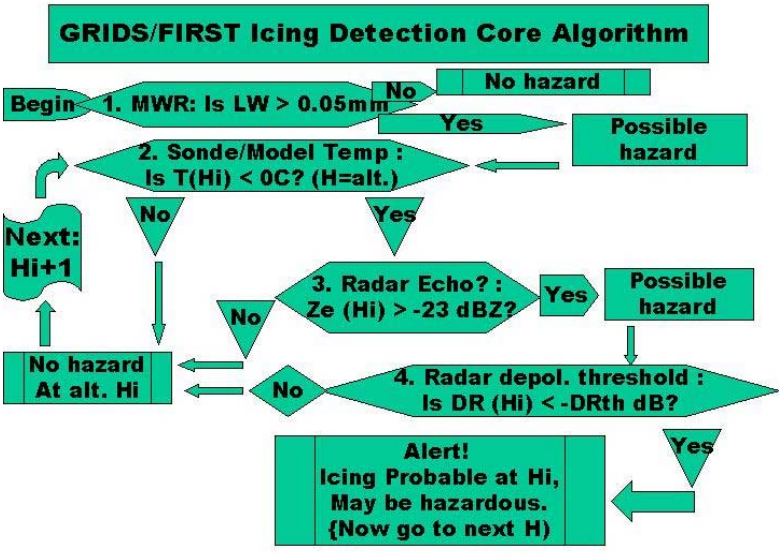

Fig. 6. Core icing hazards algorithm for Upgradable GRIDS.

A hazardous region within a cloud is identified as one that exhibits a low enough temperature ($T < 0\,^{\circ}C$), a reflectivity large enough to warrant consideration ($Z_e > -23$ dBZ), and a DR that matches the spherical hydrometeor signature (± 2 dB), all while the radiometer indicates significant liquid water along the path (LW > 0.05 mm). A reflectivity Z_e of -23 dBZ approximates that point where the minimum threshold for moderate icing conditions is met at the smallest effective droplet diameter, D_e, considered in the FAR Appendix C icing envelopes. That point is (LWC, D_e, T) = (0.3 g m^{-3}, 15 μm, 20º C). The threshold value of the depolarization ratio, DR_{th}, depends on the properties of the antenna; it will be a few decibels more than the antenna cross-talk, which is nominally specified for −30 dB. The icing potential will be indicated in a continuous time-altitude display (see **Fig. 1**) updated every minute, such that the real-time conditions and a short history (e.g., several hours) will be presented as an evolving profile through all clouds in the radar beam. The warning of icing potential will be scaled - red for probable, yellow for caution, green for no threat. The appropriate color appears at the time and altitude of the condition.

Condition Red: All four of the thresholds are affirmed.

Condition Yellow: Only the first three thresholds are met (LW > 0.05 mm, $T < 0\,^{\circ}C$, $Z_e > -23$ dBZ), but $DR > DR_{th} + 2$ dB. This indicates the co-existence of liquid and ice particles, a mixed-phase condition. Caution is warranted.

Condition Green: Clear skies obviously represent the first order condition green. Within clouds, green is established if $T > 0\,^{\circ}C$; OR if cloud is supercooled ($T < 0\,^{\circ}C$), but either LW ≤ 0.05 mm, or $Z_e \leq -23$ dBZ. Low Z_e means that the combination of droplet sizes and concentrations are insufficient to produce an icing threat, even if $DR \leq DR_{th} \pm 2$ dB. For all ice clouds $DR > DR_{th}$ and LW < 0.05 mm, establishing condition green by default.

This core algorithm for Upgradable GRIDS is conservative and may over-warn. The performance of the core algorithm will be assessed during field trials, and adjustments made later to the decision points, if needed.

4.3.2 Algorithm Enhancements.

The core algorithm can be enhanced for Target GRIDS by distributing the value of LW in different ways throughout the various portions of detected clouds, by better using temperature profiles to refine hazard potential, by using knowledge of reflectivity bright bands (if detected), and by incorporating additional information from the radar and radiometer if and when they point to the zenith. In **Appendix G** we discuss these enhancements in detail, and relate them to icing hazards potentials defined by envelopes in Appendix C of the FAR. The Target GRIDS algorithm will also be able to include adjustments of the reflectivity threshold for wet antenna and/or radome, use alternate temperature information if RUC data is unavailable, etc. The overall effect of the enhancements is to make GRIDS icing warnings more quantitative and robust.

4.4 Monitoring and Calibration

An auxiliary (AUX) computer system will be developed as a critical subsystem of GRIDS. Its primary function is to perform system health monitoring functions. Several analog and digital signals will be monitored, a radar health status log will be generated, and certain radar functions will be controlled either under human control or automatically in response to a radar system or power failure.

Industrial Packs (IPs) will be used to interface the radar system to the AUX system. IPs are small modular circuit boards that each perform a specific function. Four IP Packs are mounted on an IP carrier board which occupies one slot on the VME backplane. This technology allows the system designer to "mix and match" multiple I/O functions while using a minimum number of backplane slots. In the AUX system, an A/D IP Pack will be used to sample analog signals and digital I/O IP Packs will be used to sample and drive TTL-level digital signals. Future I/O requirements can be easily addressed by adding IP Packs with whatever functionality is needed.

The monitoring software will be written in LabVIEW. LabVIEW is a graphical programming language that is designed for instrumentation control and thus lends itself nicely to this application. LabVIEW provides a handsome graphical user interface that makes programs written in it intuitively easy to run, and results easy to interpret. LabVIEW also includes Internet support for functions such as TCP socketing, FTP file transfer, and access to Web pages. The use of these Internet functions is further discussed in the communications section of this document.

Several analog signals will be sampled hourly. Acceptable operating ranges will be established for each of these signals. Any readings that are outside the acceptable operating range will be documented and time-stamped in a status file that will be updated daily at 12:00 AM. Criteria will be established for taking action based on readings that are out of range, ranging from simple reporting within 24 hours to immediate shutdown of subsystems or entire GRIDS. For example, the radar transmitter may be automatically shut down if certain power supply failures are detected. The analog signals which will be monitored are listed in a table in the table below.

Analog Signals monitored by AUX System

CH #	I/O connector pin #	Signal Name	Units
1	1,2	Transmitted RF power	Watts
2	27,28	Outdoor temperature	Deg C
3	3,4	Outdoor humidity	Percent
4	29,30	Indoor temperature	Deg c
5	5,6	Indoor humidity	Percent
6	31,32	Pulse controller +5V #1	Volts
7	7,8	Pulse controller +5V #2	Volts
8	33,34	Pulse controller +28V	Volts
9	9,10	Pulse controller +15V	Volts
10	35,36	Pulse controller –15V	Volts
11	11,12	RF CUD +12V (mon)	Volts
12	37,38	RF CUD TX +12V (mon)	Volts

13	13,14	RF CUD RX +12V (mon)	Volts
14	39,40	IF REC/MOD +12V (mon)	Volts
15	15,16	IF REC/MOD +15V	Volts
16	41,42	Temp, circulator #1	Deg C

Digital signals to be monitored consist of phase-lock alarms on the 2.0 GHz and 16.4 GHz phase-locked-oscillators (PLO's). A course of action based on these conditions will be chosen and implemented. For example, the radar transmitter might be automatically turned off if there is a PLO failure.

Software from the UPS manufacturer will be used to monitor the incoming line power. In the event of a power failure, the AUX system will gracefully turn off the radar, radiometer, and computers in the proper sequence, before UPS power is depleted. When power is restored, the entire system will be restarted automatically and resume normal operations.

Radar and radiometer calibrations will be performed both manually and automatically. Full calibrations will be done manually at an appropriate frequency (about once per year, based on our many years' experience with such systems), or whenever failure of components dictates a recalibration. An automated verification of calibration stability will be performed daily. For this verification, two measurements will be made. First, the noise level of the receiver channel will be measured under conditions of zero transmitter power. Also, a known level of white noise will be injected into the radar receiver to produce an output near the middle of the receiver's dynamic range. Both noise levels will be recorded and compared with recent and historical values. If both values remain stable, it can be reasonably assumed that the overall receiver calibration is unchanged. To make this daily check, a digital I/O IP will be used to drive the necessary digital control signals, switching circulators and attenuators into the correct state and turning on the calibration noise diode.

4.5 Communication

4.5.1 Internet

GRADS will send a GIF (Graphical Interchange Format) file of the most recent icing hazard display via SCP (Secure Copy Program) to the Boulder Web server for display on the Web. Typically, these files will be updated and sent once per minute.

GRADS will also archive radar, radiometer, RUC, surface meteorological and icing data via SCP to the archival system in Boulder, typically once per hour.

On the AUX system, a LabVIEW program will be used to download RUC temperature profile data from the Web, as data sets become available. Typically, these data sets are updated once per hour.

A Linux firewall computer (AUX) will protect the internal GRADS (and other) systems from the

external network by providing centralized network security.

4.5.2 Local Area Network

GRADS will receive radiometer data from the Radiometer PC once per minute via a socket, and send commands to stop and start the radiometer via a TCP socket.

GRADS will send AUX system RUC data request stop/start commands via a TCP socket as necessary. On the AUX system, a LabVIEW program will be used to parse the downloaded RUC data set and extract the data needed for the icing algorithm. It will then FTP this abridged data set to a file on GRADS, where it will be available to the IDDAS. LabVIEW will also acquire surface temperature and humidity data and will send this data once a minute via a socket to GRADS for use in the icing algorithm.

LabVIEW will be used on the AUX system to send radar system status and error messages to GRADS via a TCP socket. Typical messages might notify the IDDAS that the radar has been successfully turned on, or that a hardware failure has been detected and that IDDAS should stop data acquisition.

UPS software will run on GRADS, AUX, and the Radiometer PC to monitor the UPS over a network connection. When a power failure occurs, this software will direct all three of the operating systems to shutdown gracefully. This software will also be used to send an automatic email to notify selected recipients of the problem.

4.5.3 Serial

The AUX system will communicate with the TWTA via a serial link. A LabVIEW program will be used to send commands to the TWTA and monitor its status.

The Radiometer PC will acquire data from the radiometer via a serial link.

4.5.4 VME

The UltraSPARC and the DSP board in GRADS communicate over a VME bus. The Radar Parameters file is written by the UltraSPARC into an area of memory called “slave memory” because it can be read by VME slaves. When idle, the DSP board reads this memory at a 10 Hz rate and inspects a certain word (DMOD) to see if it should begin processing. If the word is non-zero, it indicates a particular processing mode and the DSP board begins executing that mode, using the appropriate Radar Parameters to control the mode. If an error occurs, the DSP writes DMOD to zero, and sets another word (ERRC) to indicate the cause of the error. If an operator or a computer issues a stop command, the UltraSPARC will set DMOD to zero, thus halting DSP processing.

4.6 Container

Since the GRIDS prototype is to be developed in Boulder but demonstrated in other locations, it was decided to build GRIDS into a dedicated, transportable container. Because of common practice in the transportation and shipping industry, we decided to use a standard ISO shipping container for this purpose. Its dimensions are 20'L x 8'W x 8'H. This rugged steel-shelled container will also serve as a good mount for the GRIDS antenna and radiometer. It will be fitted with insulated walls, environmental controls, and a good electrical distribution system, thus providing laboratory-like conditions in which to operate. Although this system will be unattended when it is fully developed, there is still a need to make it roomy and pleasant for both visitors and project staff. Below we show the floor plan for the GRIDS container (Fig. 7), and an external side view depicting the antenna and radiometer mounted to the container (Fig. 8).

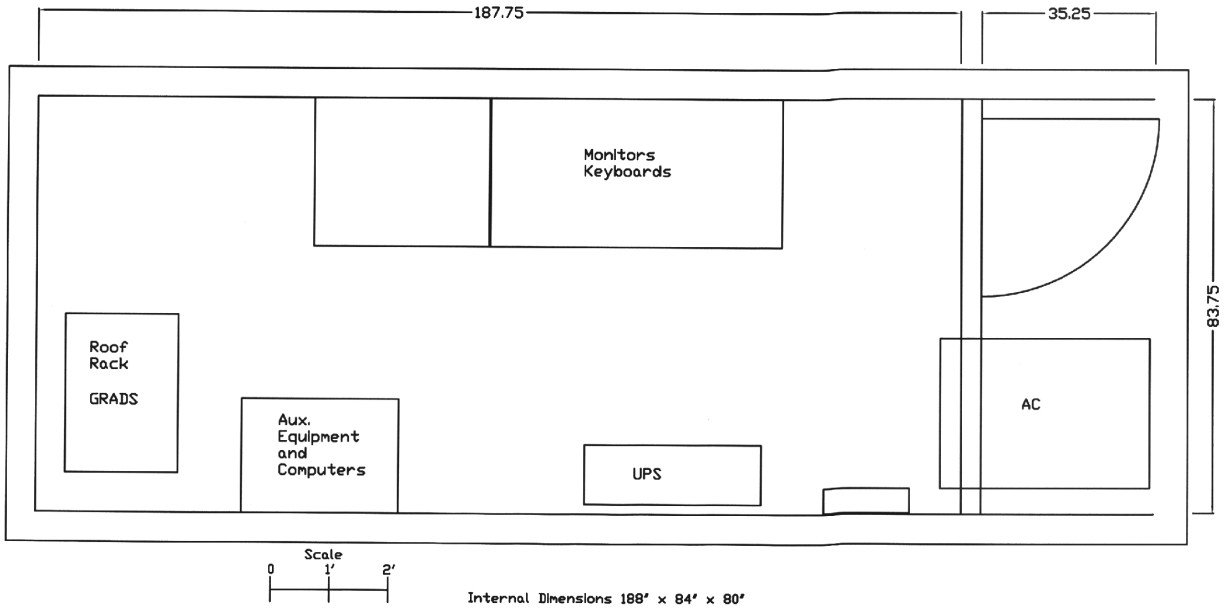

Fig. 7. Plan view of GRIDS container showing location of key equipment. Note vestibule entry.

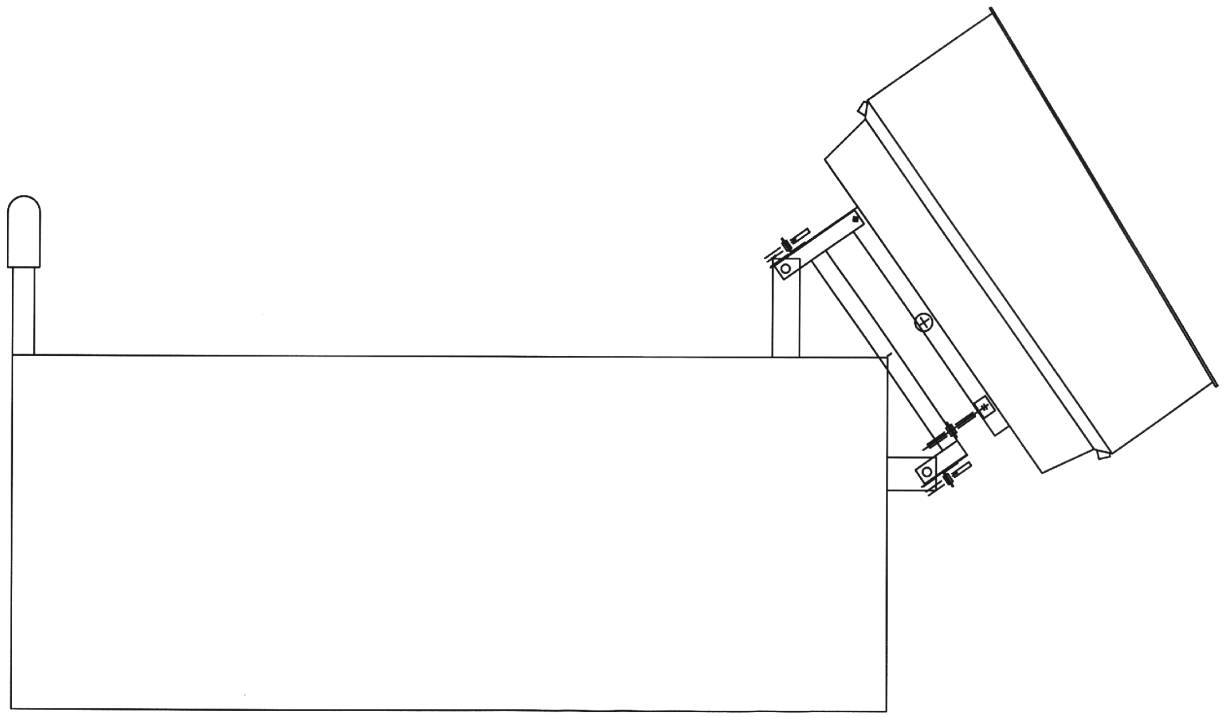

Fig. 8. Side view of container showing 3-m antenna with radome pointing at 40º elevation angle, and mailbox radiometer mounted on an opposing corner.

5.0 Test Plan

Subsystems will be tested independently as they near completion, first in the laboratory and then in the GRIDS container. Some testing began as early as July, 2001, i.e. for the radar timing generator and the auxiliary computer running LabView. As each subsystem is integrated into GRIDS, it will be further tested for functionality and compatibility with other parts of the overall system. We expect these activities to begin in April, 2002, most likely with GRIDS deployed to ETL's Erie field site about 30 km NE of Boulder. Communications with the outside world will occur over conventional lines of communication (i.e., phone line), to exercise that part of the system. Validation of GRIDS radar calibration can be made via side-by-side intercomparison with ETL's scanning Doppler K_a-band radar at Erie.

We anticipate that by October, 2002, GRIDS will be functioning at a sufficient level for shipment to Mirabel Airport near Montreal, to participate in the AIRS II campaign. AIRS II is now scheduled to begin in November 2002, and serves as the first serious application and trial of the GRIDS concept. If FAA provides sufficient supplementary funding for field operations in FY03, we intend to have ETL scientists and engineers operate Upgradable GRIDS at Mirabel.

After AIRS II, ETL will have a much better understanding of the strengths and weaknesses of this first version of GRIDS, both technically and scientifically. If any design changes are mandated, or if the icing hazards algorithms need modification or adjustment, such changes will be made in FY03. GRIDS data will be analyzed and compared with data from other systems.

In the out years (FY04 and beyond), project funds will be used by ETL to procure all critical components that have been borrowed, and to completely automate GRIDS. The resultant Target GRIDS system will then be deployed for a one-year demonstration at a site chosen by the FAA, perhaps near a Great Lakes regional airport in the U.S. that climatologically experiences a significant number of winter icing events. GRIDS outputs will be made available to appropriate controllers via the World-Wide Web, to help assess its effectiveness. The GRIDS outputs may also be used by other elements of the FAA's Product Development Team to assess and validate the results of other efforts, such as forecasting of icing conditions, ceiling, and visibility.

6.0 Budget and Schedule

Cost estimates made independently in 2000 (Kropfli) and 2001 (Post) for Target GRIDS have consistently been in the neighborhood of $1.8M. This estimate assumed that GRIDS could be built over a 2-3 year period with a nearly full-time effort by ETL staff. As detailed herein, a large part of this expense is non-recurring engineering expense, for design and software development. Hardware expenses amount to about $700K.

However, FAA cannot provide the funding to complete GRIDS in a 2-3 year timeframe. Instead it is providing about $450K per year. This approach, while completely understandable, stretches out the project more than proportionately. Limited funding means that choices must be made between buying expensive radar components and supporting people to work on the system. Neither can proceed as quickly as desired. Rather than dedicating all first-year funds to hardware, ETL has decided to buy only the more inexpensive parts (e.g., container and computing infrastructure) of the system in FY01, and to focus human efforts in FY01 on design and software. In **Appendix G** we show the MicroSoft Project Gantt chart of tasks and scheduling, based upon the preliminary design that is documented herein. As can be seen, some parts have already been purchased and work has begun on many of the sub-systems.

To accelerate the GRIDS effort towards fruition, ETL has offered to loan the project certain critical, expensive components, when ETL has access to them. Thus the concept of Upgradable GRIDS was conceived – a less than fully capable GRIDS built using borrowed components. This approach allows staff to proceed when otherwise they could not.

But there are drawbacks. The borrowed components may be recalled at any time, and for any length of time because of commitments to other programs. Inefficiencies arise that will increase overall program cost. Sporadic restarts dictated by other programs will be less efficient than a fewer number of planned pauses and resumptions. Considerable time must be spent (wasted) in extracting and reinstalling components numerous times, both on the "loaner" systems and on GRIDS. Some other efforts are also bound to be wasted because of differences between the borrowed and final GRIDS components (e.g., antenna mount, transmitter interface voltages and

signals, etc.).

While following the path to Target GRIDS through the Upgradable version, ETL continues to pursue with vigor other partners that can provide additional funding to replace the borrowed components, and hence accelerate (and make more efficient) the overall effort. These potential partners include NWS, NASA, and two groups within the U.S. Air Force. In all cases, a successful demonstration of a fully-capable GRIDS would also serve the missions of these other organizations, and their contributions would be greatly "leveraged" by FAA's primary support. Realistically, these other organizations probably cannot contribute to the GRIDS effort until FY03.

Even without immediate additional support, success of Upgradable GRIDS by FY03 will allow FAA to justify further investment to achieve full capability, through purchases of performance-enhancing components (e.g., larger transmitters, antennas, and higher throughput receivers). We summarize in an **Appendix H** table the important features and benefits of GRIDS, both in the Upgradable and Target versions.

7.0 Project Management

The GRIDS project is established with a team of twelve ETL technical and scientific experts. These team members do not work full-time on GRIDS (in general), but instead contribute to several projects over the course of a work year by working continuously for hours to weeks at a time on a given project, then switching attention to another project. Work assignments are scheduled by the division chief to derive maximum efficiency of overall staff efforts, and to "leverage" efforts among the various division projects. Such leveraging benefits GRIDS markedly; for instance, much of the GRADS development for GRIDS is paid by other agencies using the division's scanning K_a- and X-band research radars for field work.

The team meets regularly (every 3-6 weeks) to coordinate activities and to inform management of progress. Meetings of the full team or of sub-teams are called by the project manager or sub-team leaders. Currently the duty of project manager is shared by M.J. Post (Division Chief) and Timothy Schneider (staff Scientist). In addition, at least once a month Schneider polls all team members asking for accomplishments in writing, which he subsequently plots on a Gantt chart. Roger Reinking, Project Leader, provides scientific direction and planning, reports to the FAA and the applications and scientific communities on project activities, and develops partnerships with other agencies. Reinking and Post/Schneider establish spending and work guidelines for the team, based on discussions with Marcia Politovich (PDT Lead) and David Pace (FAA PDT Coordinator). Below we list current team members alphabetically, together with skills and years of experience. Each has contributed to this document.

Person	Major Skills	Years Experience
T. Ayers	Electronic Technician	8
B.W. Bartram	Electronic Engineer (Radar, Programming)	25
C. Campbell	Electronic Engineer (DSP, Radar)	25
K.A. Clark	Electronic Engineer (Radar, Programming)	20
J.S. Gibson	Computer Specialist (Real-Time Systems)	20
D.A. Hazen	Electronic Engineer (Radiometer, Radar)	20
W.B. Madsen	Computer Specialist (Systems Design)	15
S.Y. Matrosov	Physicist, Theory and Data, Radar Meteorology	15
K.P. Moran	Electronic Engineer (Radar)	30
M.J. Post	Supervisory Physicist	30
R.F. Reinking	Radar Meteorologist	30
T. Schneider	Physicist, Radar Meteorology	5

Acknowledgments

FAA supports ETL in its development of GRIDS, including this design work. This document satisfies the requirements of In-flight Icing PDT (#4), Technical Direction, FY01, namely 01.4.3.2 Ground-based Remote Icing Detection System (GRIDS), FAA Icing Remote Sensing Testbed (FIRST), Deliverable 01.4.3.2.E2 Sep '01 (Formal Engineering Preliminary Design Review Document for GRIDS/FIRST). The views expressed are those of the authors and do not necessarily represent the official policy or position of the FAA.

REFERENCES

A Bibliography of NOAA/ETL Publications Establishing the Foundation of GRIDS (in chronological order)

Westwater, E. R., 1972: Microwave emission from clouds. NOAA TR ERL 219-WPL 18, 43 pp. [Avail. from Supt. of Documents, U.S. Gov't. Printing Office, Washington, DC 20402.]

Hogg, D.C., F.O. Guiraud, J.B. Snider, M.T. Decker, and E. R. Westwater, 1983: A steerable dual-channel microwave radiometer for measurement of water vapor and liquid in the troposphere. *J. Cli. Appl. Meteorol.*, *22,* 789-806.

Popa Fotino, I.A., J.A. Schroeder, and M.T. Decker, 1986: Ground-based detection of aircraft icing conditions using microwave radiometers. *IEEE Trans. Geosci. Remote Sens.,* **GE-24**, 6, 975-982.

Martner, B.E., R.A. Kropfli, L.E. Ash, and J.B. Snider, 1991: Progress report on analysis of differential attenuation radar data obtained during WISP-91. *NOAA Tech. Memo.*, ERL WPL-215, Boulder, CO, 43 pp.

Matrosov, S. Y., 1991a: Theoretical study of radar polarization parameters obtained from cirrus clouds. *J. Atmos. Sci.,* **48,** 1062-1070.

Matrosov, S. Y., 1991b: Prospects for the measurement of ice cloud particle shape and orientation with elliptically polarized radar signal. Radio Sci., 26, 847-856.

Politovich, M.K., B.B. Stankov, and B.E. Martner, 1992: Use of combined remote sensors for determination of aircraft icing altitudes. *Preprints, 11th Intl. Conf. on Clouds & Precip.*, Montreal, Canada, ICCP, 979-982.

Rasmussen, R. M. Politovich, J. Marwitz, W. Sand, J. McGinley, J. Smart, R. Pielke, S. Rutledge, D. Wesley, G. Stossmeister, B. Bernstein, K. Elmore, N. Powell, E. Weswater, B. Stankov, and D. Burrows, 1992: Winter Icing and Storms Project (WISP), *Bull. Amer. Meteorol. Soc.,* **73,** 951-974.

Matrosov, S.Y., and R.A. Kropfli, 1993: Cirrus cloud studies with elliptically polarized K_a-band radar signals: A suggested approach. J. Atmos. and Oceanic. Technol., 10, 684-692.

Stankov, B.B., B.E. Martner, J.A. Schroeder, M.K. Politovich, and J.A. Cole, 1993: Liquid water and water vapor profiling in multi-layered clouds using combined remote sensors. Paper AIAA 93-0395, *Reprints, 31st Aerospace Sciences Mtg.*, Reno, AIAA, 8pp.

Martner, B.E., and R.A. Kropfli, 1993: Observations of multi-layered clouds using K-band radar. Paper AIAA 93-0394, *Reprints, 31st Aerospace Sciences Mtg.*, Reno, AIAA, 8pp.

Martner, B.E., R.A. Kropfli, L.E. Ash, and J.B. Snider, 1993a: Dual-wavelength differential attenuation radar measurements of cloud liquid water content. *Preprints, 26th Intl Conf. on Radar Meteor.*, AMS, Norman, OK, 596-598.

Martner, B.E., R.A. Kropfli, L.E. Ash, and J.B. Snider, 1993b: Cloud liquid water content measurement tests using dual-wavelength radar. NOAA Tech. Memo.. ERL ETL-235, NOAA Environmental Research Laboratories, Boulder, CO, 47 pp.

Reinking, Roger F. Brad W. Orr, Boba Stankov, and Christopher Davis, 1993: NOAA K_a-band cloud-sensing radar measurements from WISPIT. *Preprints, 5th International Conference on Aviation Weather Systems*, 2-6 August 1993, Vienna, VA. American Meteorological Society, Boston, MA, 130-134.

Frisch, A.S., C.W. Fairall, and J.B. Snider, 1995: Measurement of cloud and drizzle parameters in ASTEX with Ka-band Doppler radar and a microwave radiometer. *J. Atmos. Sci.,* **52**, 2788-2799.

Orr, B.W., and B.E. Martner, 1995: Detection of weakly precipitating winter clouds by a NOAA 404 MHz wind profiler. *J. Atmos. & Oceanic Tech.*, **13**, 570-580.

Politovich, M.K., B.B. Stankov, and B.E. Martner, 1995: Determination of liquid water altitudes using combined remote sensors. *J. Appl. Meteor.*, **35**, 2060-2075.

Kropfli, R.A., S.Y. Matrosov, T. Uttal, B.W.Orr, A.S. Frisch, K.A. Clark, B.W.Bartram, R.F.Reinking, J.B. Snider, and B.E. Martner, 1995: Cloud physics studies with 8 mm wavelength radar. Special issue on cloud microphysics and applications to global climate change, *Atmospheric Research*, **35,** 299-313.

Gibson, J.S., and B.E. Martner, 1995: Interactive auxiliary real-time data system for NOAA/ETL Doppler radars. *Preprints, 11th Intl. Conf. on Interactive Info. Processing Systems for Meteor., Ocean., and Hydrology*, Dallas, AMS, 304-309.

Matrosov, Sergey Y., Roger F. Reinking, Robert A. Kropfli, and Bruce W. Bartram, 1995: Identification of ice hydrometeor types with elliptical polarization radar measurements. *Preprints, 27th Conference on Radar Meteorology*, 9-13 October 1995, Vail, Colorado. American Meteorological Society, Boston, MA, 539-541.

Reinking, Roger F., Sergey Y. Matrosov, Brooks E. Martner, Robert A. Kropfli, and Bruce W. Bartram, 1995a: Hydrometeor identification with millimeter-wave dual-polarization radar. *Conference on Cloud Physics*, 15-20 January 1995, Dallas, Texas. Amer. Meteorol. Soc., Boston, MA, 20-25.

Reinking, Roger F., Sergey Y. Matrosov, Roelof J. Bruintjes, Brooks E. Martner, and Robert A. Kropfli, 1995b: Further comparison of experimental and theoretical radar polarization signatures due to ice hydrometeor shape. *Preprints, 27th Conference on Radar Meteorology*, 9-13 October 1995, Vail, Colorado. American Meteorological Society, Boston, MA, 47-49.

Kropfli, R.A., and R.D. Kelly, 1996: Meteorological research applications of mm-wave radar. *Meteorol. and Atmos. Phys.,* **59,** 105-121.

Matrosov, S.Y., R.F. Reinking, R.A. Kropfli, and B.W. Bartram, 1996a: Estimation of hydrometeor shapes and types from radar polarization measurements. *Journal of Oceanic and Atmospheric Technology*, **13,** 85-96.

Reinking, Roger F., Sergey Y. Matrosov, and Reolof T. Bruintjes, 1996a: Ice and water hydrometeor identification with elliptical polarization radar: Applications to precipitation enhancement. *Preprints, 13th Conference on Planned & Inadvertent Weather Modification*, 28 January-2 February, 1996, Atlanta, GA. Amer. Meteor. Soc., Boston, MA, 172-179.

Reinking, Roger F. Sergey Y. Matrosov, and Roelof T. Bruintjes, 1996b: Hydrometeor identification with elliptical polarization radar: Applications for glaciogenic cloud seeding. Cover article, *Journal of Weather Modification*, **28,** 6-18.

Reinking, Roger F., Sergey Y. Matrosov, Brooks E. Martner and Robert A. Kropfli, 1996c: Differentiation of freezing drizzle from ice hydrometeors and rain with polarization radar. *Proceedings, FAA International Conference on Aircraft Inflight Icing*. 6-8 May 1996, Springfield, VA, **II,** 331-338. [Available from NTIS, Springfield, VA 22161. DOT/FAA/AR-96/81].

Reinking, Roger F., Sergey Y. Matrosov, Brooks E. Martner and Robert A. Kropfli, 1996d: Differentiation of freezing drizzle from ice hydrometeors with polarization radar. *Proceedings, 12th International Conference on Clouds and Precipitation.* 19-23 August 1996, Zurich, Switzerland. International Commission on Clouds and Precipitation (ICCP); **I,** 446-449.

Reinking, Roger F., Sergey Y. Matrosov, Brooks E. Martner, Robert A. Kropfli, and Bruce W. Bartram, 1996e: Hydrometeor identification with millimeter-wave dual-polarization radar. *Proc. ETL/CSU Cloud-related Process Modeling and Measurement Workshop, Boulder, Colorado, 23-25 October 1995.* Environmental Technology Laboratory, U.S. Dept. of Commerce, 209-214.

Reinking, Roger F., Sergey Y. Matrosov, Roelof J. Bruintjes, Brooks E. Martner, and Robert Kropfli, 1996f: Further comparison of experimental and theoretical radar polarization signatures due to ice hydrometeor shape. *Proc. ETL/CSU Cloud-related Process Modeling and Measurement Workshop, Boulder, Colorado, 23-25 October 1995.* Environmental Technology Laboratory, U.S. Dept. of Commerce, 215-218.

Campbell, W.C., and J.S. Gibson, 1997: A programmable real-time data processing and display system for the NOAA/ETL Doppler Radars. Preprints, 28th Conf. Radar. Meteorology, Austin, TX, Amer. Met. Soc., 178-179.

Reinking, Roger F., Sergey Y. Matrosov, Roelof T.Bruintjes, and Brooks E. Martner, 1997a: Identification of hydrometeors with elliptical and linear polarization K_a-band radar. *Journal of Applied Meteorology*, **36**, 322-339.

Reinking, Roger F., Sergey Y. Matrosov, Brooks E. Martner, and Robert A. Kropfli, 1997b: Differentiation of freezing drizzle from ice hydrometeors and freezing rain with dual-polarization radar. *Journal of Aircraft*, **34**, 778-784.

Reinking, Roger F., 1997c: Hydrometeor and dispersion measurements with 3-cm and 8-mm dual-polarization radar. Proceedings, WMO Workshop on Cloud Properties for Forecasts of Weather and Climate. 23-27 June 1997. Mexico City, Mexico. WMO TD No. 852, 255-269.

Reinking, Roger F., 1998: Detection of ice hydrometeors and freezing drizzle with K_a-band dual-polarization radar. *Conference on cloud physics. 17-21 August 1998, Everett, Washington.* Amer. Met. Soc., Boston. Pp 249-252.

Klimowski, B.A., R. Becker, E.A. Betterton, R. Bruintjes, T. L. Clark, W. D. Hall, B. W. Orr, R. A Kropfli, P. Piironen, R. F. Reinking, D. Sundie, and T. Uttal, 1998: The 1995 Arizona Program: Toward a better understanding of winter storm precipitation development in mountainous terrain. *Bul. Amer. Meteorol. Soc*, **79,** 799-813.

Matrosov, S.Y., A.J. Heymsfield, R.A. Kropfli, B.E. Martner, R.F. Reinking, J.B. Snider, P. Piironen, and E.W. Eloranta, 1998: Comparisons of ice cloud parameters obtained by combined remote sensor retrievals and direct methods. *Journal of Atmospheric and Oceanic Tech.,* **15,** 184-196.

Kropfli, Robert A., Brooks E. Martner, Sergey Y. Matorsov, Roger F. Reinking, A.Shelby Frisch, and Taneil Uttal, 1998: Radar and radiometer measurements of the physical parameters of clouds and precipitation at the NOAA Environmental Technology Laboratory. *Proc. Conf. on Battlespace Atmospheric and Cloud Impacts on Military Operations (BACIMO).* Hanscom AFB, MA, 1-3 Dec 1998, 125-132.

Moran, K.P., B.E. Martner, M.J. Post, R.A. Kropfli, D.C. Welsh, and K.B. Widener, 1998: An unattended cloud-profiling radar for use in climate research. *Bull. Amer. Meteor. Soc.*, **79**, 443- 455.

Reinking, R.F., S.Y. Matrosov, B. E. Martner, B.W. Orr, R.A. Kropfli, and B.W. Bartram, 1999: Slant-linear polarization applied to detection of supercooled drizzle. *Preprints, 29th Conf. on Radar Meteorology,* Montreal, Canada, 285-288.

Reinking, R.F., 1999: Influence of ice particles on remote detection and assessment of atmospheric supercooled liquid water. Proceedings, FAA Specialists' Workshop on Mixed-phase and Glaciated Icing Conditions, 2-3 December 1998, Atlantic City, NJ, Editors, James T. Riley and Rosemarie McDowall. FAA Technical Center, Atlantic City, pp. 303-304.

Vivekanandan, J., B.E. Martner, M.K. Politovich, and G. Zhang, 1999: Aircraft icing detection using dual-wavelength radar observations. *IEEE Trans. Geosci. & Remote Sensing*, 2325-2334.

Frisch, A.S., B.E. Martner, I. Djalalova, and M.R. Poellot, 2000: Comparison of radar/radiometer retrievals of stratus cloud liquid water content profiles with in-situ measurements by aircraft. *J. Geophys. Res.,* **105**, 15361-15364.

Moran, K.P., B.E. Martner, and H.A. Winston, 2000: Dual-polarization and processor efficiency enhancements of the DOE's millimeter-wavelength cloud radars (MMCR). *Reprints, TECO-2000, WMO Tech. Conf. on Meteor. & Environ. Instruments and Methods of Observation*, Beijing, China, 4 pp.

Reinking, Roger F., Jack B. Snider, and Janice L. Coen, 2000a: Influences of storm-embedded orographic gravity waves on cloud liquid water and precipitation. *J. Appl. Meteor.,* **39,** 733-759.

Ryerson, Charles C., Marica K. Politovich, Kenneth L. Rancourt, George G. Koenig, Roger F. Reinking, and Dean R. Miller, 2000: Mt. Washington Icing Sensors Project: Conduct and Preliminary Results. *Paper # AAIA-2000-0488, Preprints, 38th AAIA Aerospace Sciences Meeting and Exhibit*, 10-13 January 1999, Reno, Nevada, 10 pp.

Reinking, R.F., B.W. Orr, L. R. Bissonnette, G. Roy, and A. S. Frisch and S. Y. Matrosov, 2000b: Remote sensing of cloud droplets during MWISP. Proceedings, Intn'l. Geoscience and Remote Sensing Symposium (IGARSS 2000). Honolulu, HI, 24-28 July 2000. Pp 187-189. (Available from customer.services@ieee.org).

Matrosov, S.Y., R.F. Reinking, R.A. Kropfli, B.E. Martner, and B.W. Bartram, 2000c: Inferring hydrometeor shapes using different polarization states of radar signals. Proceedings Intn'l. Geoscience and Remote Sensing Symposium (IGARSS 2000). Honolulu, HI, 24-28 July 2000. Pp. 1577-1579. (Available from customer.services@ieee.org.)

Reinking, R.F., S.Y. Matrosov, B.W. Bartram, and R.A. Kropfli, 2000d: Evaluation of a slant-45-quasi-linear polarization state for distinguishing among drizzle droplets and quasi-spherical ice particles. *Preprints, International Conference on Cloud Physics*, Reno, NV, 14-18 Aug 2000. Pp. 243-246. (Avail. from Desert Research Inst., 2215 Raggio Parkway, Reno, NV.)

Reinking, R.F., S.Y. Matrosov, C.C. Ryerson, R. A. Kropfli, and B. W. Bartram, 2000d: Verified detection of supercooled large droplets with dual-polarized, millimeter-wave radar. *Ninth Conf. on Aviation, Range, and Aerospace Meteorology,* 11-15 Sept. 2000, Orlando Fla. Amer. Meteor. Soc., Boston. 537-542.

Reinking, R.F., and R.A. Kropfli, 2000: Breakthroughs in radar polarization technology and related studies. Radar-based Icing Diagnosis Techniques, In-flight Icing PDT Technical Direction FY2000 Year0end Task Progress Report to the FAA, Deliverable 00.4.3.E1. NOAA Environmental Technology Laboratory. 16 pp.

Matrosov, S.Y., R.F. Reinking, R.A. Kropfli, B.E. Martner, and B.W. Bartram, 2001: On the use of radar depolarization ratios for estimating shapes of ice hydrometeors in winter clouds. *J. Appl. Meteorol.,* **40,** 479-490.

Reinking, R.F., R.A. Kropfli, S.Y. Matrosov, W. C. Campbell, M.J. Post, D. A. Hazen, J.S. Gibson, K.P. Moran, and B.E. Martner, 2001a: Concept and Design of a Pilot Demonstration Ground-based Remote Icing Detection System. *Proceeding 30th International Conference on Radar Meteorology,* 19-24 July, Munich. Amer. Meteor. Soc., Boston, 199-201.

Reinking, R.F., R.A. Kropfli, S.Y. Matrosov, W. C. Campbell, M.J. Post, D. A. Hazen, J.S. Gibson, K.P. Moran, B.E. Martner, and T. Schneider, 2001b: Concept and Design of a Pilot Demonstration Ground-based Remote Icing Detection System. *Proc. Conf. on Battlespace Atmospheric and Cloud impacts on military operations (BACIMO)*. July, Ft. Collins, CO.

Reinking, R.F., S.Y. Matrosov, B.W. Bartram, and R.A. Kropfli, 2002: Evaluation of a 45°-slant quasi-linear radar polarization state for distinguishing drizzle droplets, pristine ice crystals, and less regular ice particles. *Journal of Atmospheric and Oceanic Technology* (in press).

Martner, B.E., B.W. Bartram, J.S. Gibson, W. C. Campbell, R. F. Reinking, and S.Y. Matrosov, 2002: An overview of NOAA/ETL's scanning K_a-band cloud radar. 16th Conf. on Hydrology. Jan 2002, Orlando, Fla. Amer. Meteor. Soc. (in press).

Martner, B.E., D.A. Hazen, K.P. Moran, T. Uttal, M.J. Post, and W. B. Madsen, 2002: NOAAETL's vertical-profiling cloud radar and radiometer package. 6th Symp. on Integrated Observing Systems, Jan 2002, Orlando, FL, Amer. Meteor. Soc. (in press)

ADDITIONAL REFERENCES
(in aphabetical order)

Ashendon, R., W. Lindberg, J. Marwitz, and B. Hoxie, 1996: Airfoil performance degradation by supercooled cloud, drizzle, and rain drop icing. *J. Aircraft*, **33**, 1040-1046.

Ashendon, R., and J. D. Marwitz, 1997: Turboprop aircraft performance response to various environmental conditions. *J. Aircraft*, **34**, 278-287.

Brandes, E. A., and M. K. Politovich, 1999: the potential for aircraft icing detection with polarimetric radar. Report prepared for the Federal Aviation Administration (18 June), NCAR, 14 pp.

Cober, S. G., "G. Isaac, and J. W. Strapp, 1995: Aircraft icing measurements in east coast winter storms, *J. Appl. Met.,* **34,** 88-100.

Doviak, R. J., V. Bringi, A. Ryzhkov, A. Zahrai, and D. Zrnić, 2000: Considerations for polarimetric upgrades to operational WSR-88D radars. J. Atmos. Oceanic Tech., **17,** 257-278.

Federal Aviation Regulations, 1982: Part 25: Airworthiness standards, transport category airplanes (revised edition). Icing FAR's: Parts 25--Appendix C, 91.527, 121.629, 125.221, 135.227. Federal Aviation Administration. U.S. GPO, Wash., D.C.

Hunter, S.M., E.W. Holroyd, and C.L. Hartzel, 2001: Improvements to the WSR-88D snow accumulation algorithm. *Preprints, 30th Intl. Conf. on Radar Meteorology*, Munich, Germany, Amer. Meteor. Soc., 716-718.

McDonough, F. and B.C. Bernstein, 1999: Combining satellite, radar, and surface observations with model data to create a better aircraft icing diagnosis. *Preprints, 8th Conference on Aviation*, Range and Aerospace Meteorology, Dallas TX, Amer. Meteor.Soc., 467-471.

Paull, G. and E. Hagy, 1999: Historical overview of in-flight icing accidents. TR-9854/01-1 MCR Federal, Inc. Bedford MA 01730. 43 pp.

Politovich, M. K., 1989: Aircraft icing caused by large supercooled droplets. *J. Appl. Met.*, **28**, 856-868.

Politovich, M. K, 1996: Response of a research aircraft to icing and evaluation of Severity Indices. *J. Aircraft*, **33**, 291-297.

Riley, J., and B. Horn, 1996: Plenary sessions. Proc. FAA Intn'l. Conf. Aircraft Inflight icing. DOT/FAA/AR-96/81, I, 263 pp. (Available from NTIS, Springfield VA 22161.)

Sand, W. R., A. Cooper, M. K. Politovich, and D. L. Veal, 1984: Icing Conditions encountered

by a research aircraft. J. Cli. & Appl. Met., 1427-1439.

Schultz, P., and M.K. Politovich, 1992:Toward the improvement of aircraft-icing forecasts for the continental united States. *Wea. and Forecasting,* **7,** 491-500.

Zawadski, I., W. Szyrmer, and S. Laroche, 2000: Diagnostic of supercooled clouds from single-Doppler observations in regions of radar-detectable snow. *J. Appl. Met.,* **39,** 1041-1058.

APPENDIX A

History of Icing Hazards Research at NOAA/ETL

Instruments	Started	Use, Tests, Key References
Microwave Radiometer	1983	Measure vertical liquid water path; correlate with icing pireps and aircraft incidents (e.g. Popa Fotino *et al.*1986; Stankov *et al.* 1992).
Cloud Radar	1991	Determine cloud layer altitudes and internal structure with high resolution (*e.g.* Martner and Kropfli 1993).
Microwave Radiometer + Cloud Radar	1993	Estimate vertical profile of liquid within cloud layers; compare with aircraft soundings of liquid (Politovich *et al.* 1995; Frisch *et al.* 1995).
Unattended, Zenith-pointing Cloud Radar	1996	Continuous monitoring of altitudes and internal structure of clouds overhead (Moran *et al* 1998; Martner *et al.* 2002).
Dual-wavelength Radar	1991	Measure liquid water content of clouds and map it in 3-D; comparisons with liquid path of steerable microwave radiometer (Martner *et al.* 1991 and 1993).
Dual-polarization Cloud Radar	1991	Identify hydrometeor types; comparison with scattering theory and in situ particle sampling (e.g. Matrosov 1991, Matrosov et al. 1996, Reinking et al. 1997a,b, Matrosov et al. 2001, Reinking et al. 2000, 2002)

ETL=s earliest icing research used ground-based dual-frequency (near 20- or 23-GHz and 31-GHz) microwave radiometers to monitor the liquid water path overhead and correlated those measurements with nearby pilot reports (Westwater 1972, Hogg et al. 1983, Popa Fotino et al. 1986, Stankov et al. 1992). A few years later, ETL developed a scanning millimeter-wave Doppler cloud radar (35-GHz, K_a-band) which has evolved into a powerful research tool (Kropfli et al. 1995, Kropfli and Kelly 1996). This radar uses a much shorter wavelength (8.66 mm) than conventional weather surveillance radars (typically 5 or 10 cm), to more readily detect tiny cloud droplets and ice crystals, in addition to the larger raindrops and snowflakes. Thus clouds themselves, and not just precipitation, are observed.

Vertically-pointing cloud radar delineates cloud layer boundaries and internal reflectivity and

velocity structure with remarkable detail, accurately defining cloudy and cloud-free (hence, icing-free) altitudes aloft (Martner and Kropfli 1993). A logical step was to combine the radiometer=s path-integrated liquid measurements with the cloud radar=s range-resolved observations of cloud structure and boundaries, to allow vertical profiles of liquid within cloud layers to be estimated (Politovich et al. 1995, Frisch et al. 1995).

Unattended, continuous monitoring of cloud layer heights and structure became available at in 1996 with ETL=s development of a vertically-pointing version of the scanning radar (Moran et al. 1998, Martner et al. 2002). That Millimeter-wave Cloud Radar (MMCR), as well as other remote sensing systems, gave ETL experience in building unattended, nearly operational systems. The MMCR now provides 24/7/365 measurements at several DOE CART (Clouds and Radiation Testbed) sites world-wide.

In 1991 and 1999 NOAA/ETL attempted to combine data from a second radar (X-band, 9.3 GHz or 3.1 cm) with its K_a-band radar data to test a dual-wavelength differential-attenuation method for measuring the three-dimensional distribution of liquid water content in clouds. The shorter wavelength K_a-band signal is more strongly attenuated than the longer wavelength, and in theory the wavelength attenuation difference is directly related to the cloud liquid water content. Tests, however, revealed that practical problems (e.g., antenna sidelobes and ground clutter) and natural cloud conditions (e.g., variations in size distribution) disrupt this relationship and make the liquid content estimation dubious under many circumstances (Martner et al. 1991, 1993; Vivekanandan et al 1999). Hence ETL abandoned the dual-wavelength approach to icing detection because it appeared to have too many practical problems, including the need to precisely match radar sensing volumes while maintaining sufficient sensitivity at useful ranges.

In 1991 NOAA/ETL also began to explore the utility of dual-polarization methods, both theoretically and with its K_a-band radar. The theoretical work focused on various observational techniques to distinguish the many types of ice particles in cirrus clouds, for climate studies. A key advance was the prediction, and subsequent confirmation, that the depolarization ratio of different ice and water hydrometeors in clouds varies markedly with elevation angle (Matrosov 1991a,b; Matrosov and Kropfli 1993). DuringWISP it was shown that measurements of depolarization by various types of ice particles could be used to identify them. In fact, hydrometeor evolution could be followed in winter storms (Reinking et al. 1993, 1995a,b, 1996a; Matrosov et al. 1995, Matrosov et al 1996a). Whereas drizzle-sized droplets were initially used only for calibration, it was quickly realized that the depolarization measurements could be used to distinguish all spherical (liquid) cloud droplets, including SLD, from ice crystals (Reinking et al. 1996b-e, 1997a,b).

Henceforth, ETL=s most important on-going task for the FAA became the development of a dual-polarization K_a-band radar to detect clouds of hazardous SLD, and to distinguish them from clouds with non-hazardous ice particles. Supporting theory was improved (Matrosov et al. 1996a, 2000, 2001; Reinking et al. 1997a, 2002), and in a long series of intensive tests culminating with MWISP, ETL was able to demonstrate a remote capability for deterministic hydrometeor identification using the pattern of depolarization-ratio vs. elevation-angle. These remotely-sensed radar results were corroborated by direct detection of cloud particles and

precipitation by other means (e.g., aircraft and mountain-top in situ sensors). (Matrosov et al. 1996a, 2001; Reinking et al. 1997a,b, 1998, 2000a-c, 2002).

This excellent and repeatable agreement between theory, measurement, and independent validation thus pointed the way to the design for an operational system of integrated sensors for detecting icing conditions aloft, which is GRIDS (Reinking and Kropfli 2000, Reinking et al. 2001a,b).

APPENDIX B

GRIDS Requirements

1. Description

GRIDS (Ground-based Remote Icing Detection System) is an autonomous and reliable pilot demonstration radar/radiometer system whose purpose is to detect, from the ground, icing conditions that are hazardous to aircraft. To accomplish this, it transmits a K_a-band circularly polarized signal (the co-polarized signal) and receives a co-polarized and cross-polarized signal sequentially, using a fixed pointing angle of about 40 degrees. Icing conditions are detected using an algorithm that utilizes the depolarization ratio between the co-polarized and cross-polarized channels, the absolute reflectivity from the co-polarized channel, information from the dual-channel radiometer, local surface temperature and humidity, and temperature profiles from the RUC (Rapid Update Cycle) model obtained via the Internet. GRIDS will run continuously while unattended and transmit data over the Internet for archival at ETL. A display indicating the possibility of aircraft icing will be served over the Internet and will be accessible with common Web browser software.

Functionally, GRIDS consists of a container system (a seatainer), a radar system, a radiometer system and a data processing system. Two-way Internet communications are needed to ingest model temperature data and to communicate warnings, data and system health information to the outside world. The radar system consists of the radar transmitter, radar receiver and antenna. The radiometer system consists of a dual-channel, liquid/vapor microwave radiometer.

This document describes requirements for a base system and for desirable options. Options include a scanning antenna (in elevation) which would allow zenith-pointing data, a dual receiver (so co-polar and cross-polar data may be acquired simultaneously resulting in a 3 dB increase in sensitivity) and spectral processing. Spectral processing is necessary to effectively utilize zenith-pointing data; it would also increase sensitivity somewhat.

2. GRIDS Requirements

2.1. Container and environmental requirements

2.1.1. The GRIDS shall be housed in a seatainer of dimensions 8’6” H x 8’ W x 20’ L.

2.1.2. The GRIDS shall be capable of being transported by flat bed semi-trailer (min. 30 ft long, oversize load due to the antenna).

2.1.3. The GRIDS shall operate on single-phase, 240 VAC power, center-tapped, at 60 Hz.

2.1.4. The GRIDS shall operate over an ambient temperature range of -20 deg C to +40 deg C.

2.2. Radar requirements

2.2.1. The radar shall operate in the Ka band at about 35 GHz.

2.2.2. The radar shall transmit a single circular polarization and receive sequentially that polarization (co-polarization) and the orthogonal polarization (cross-polarization).

2.2.3. The radar transmitter shall use a TWTA.

2.2.4. The radar receiver shall receive sequentially the co-polar and cross-polar channel on a pulse-to-pulse basis, and provide an in-phase and quadrature-phase output at baseband.

2.2.5. The radar shall meet the performance requirements indicated in Table 1.

2.2.6. The receiver bandwidth shall be determined by two matched filters that are switchable to match the following transmit pulse widths: 1.00 μsecs and 1.55 μsecs.

2.2.7. The antenna shall be manually adjustable, in less than one day, from 30 to 90 degrees. The nominal pointing angle is 40.2 degrees. The design shall allow for motor adjustment in less than 1 minute between 40.2 degrees and 90.0 degrees.

Parameter	Min	Nominal	Max	Units	Comment
Transmit frequency	34.5	34.86	35.5	GHz	
Transmit tube lifetime		20000		hours	
Pulse repetition period	50		150	μsecs	
Peak transmit power		1000		watts	
Duty cycle			15%		
Transmit pulse width	0.05	2.0	10	μsecs	
Receiver noise floor		-105	-100	dBm	
Antenna diameter		3		meters	
Antenna elevation	30	40.2	90	degrees	mechanically adjustable
Antenna elevation	30		90	degrees	scanning option
Antenna beamwidth		0.2		degrees	circular beam
Antenna cross-polar isolation	30			dB	as measured on antenna range
Antenna gain	57			dB	

Table 1. Radar specifications.

2.3. Radiometer system requirements

2.3.1. The radiometer system shall consist of a dual-channel microwave radiometer meeting the specifications shown in Table 2.

2.3.2. The radiometer shall be mounted on the GRIDS container.

2.3.3. The radiometer shall be capable of being adjusted to selected fixed elevations, or scanned in elevation to match the positioning options for the radar.

2.3.4. The microwave radiometer shall perform auto-calibrations at regular intervals.

2.3.5. The dual-channel radiometer shall transmit data to the RADS.

Parameter	Min	Nominal	Max	Units	Comment
Frequencies		23.8 31.6		GHz	
Bandwidth		400		MHz	
Antenna beam width		5.7		degrees	
Accuracy		0.5		degrees K	
Operating temperature	-20		+50	C	

Table 2. Liquid/vapor radiometer specifications.

2.4. GRIDS Radar Acquisition and Data System (RADS) requirements

2.4.1. GRADS shall support unattended operation by executing operator-defined queues of operating parameters, and by allowing remote (via Internet) monitoring of its operation.

2.4.2. GRADS shall process radar data in real-time in a covariance (pulse-pair) mode, and calculate, as a minimum, the fields shown in Table 3. DC correction shall be applied.

Field	From co-polar channel	From cross-polar channel	From both channels	Units	Purpose
Velocity	Vc	Vx		m/s	diagnostic
Width	Wc	Wx		m^2/s^2	diagnostic
Correlation	Cc	Cx		None	diagnostic
Intensity (power at receiver output)	Ic	Ix		dBm	diagnostic
Power received (at antenna terminals)	Pc	Px		dBm	diagnostic
Reflectivity	Zc	Zx		dBZ	algorithm
Depolarization ratio			DR	dB	algorithm

Table 3. Moment data fields.

2.4.3. GRADS shall be capable of performing spectral processing of time series data, as an option.

2.4.4. GRADS shall be capable of displaying data fields from the covariance method in a time-range (A-scope) format.

2.4.5. GRADS shall be capable of performing a receiver calibration verification at scheduled intervals.

2.4.6. GRADS shall be capable of saving covariance data to tape.

2.4.7. GRADS shall resume scheduled activity without operator intervention following a power failure.

2.4.8. GRADS shall ingest temperature profile data from external sources via the Internet for the purpose of determining the freezing level. The system will be able to obtain temperature data accurate to one degree Celsius from ground level to ten km in altitude, once per hour for a point within 40 km radius with a vertical resolution between 100 and 300 meters.

2.4.9. The data processing system shall run unattended with no local operator intervention except for maintenance.

2.4.10. The system shall be capable of operating during a power outage that does not exceed 15 minutes. If the power outage exceeds the power backup capability, the system shall shut down and recover automatically when power is restored, resuming all scheduled operations.

2.4.11. The system shall be capable of recovering automatically from environmental under- temperature and over-temperature conditions.

2.4.12. GRADS shall integrate radar, radiometer, and temperature data and execute an icing detection algorithm in real time.

2.4.13. GRADS shall provide an easy-to-interpret time-height display of icing conditions within clouds, possibly based on a green-yellow-red color scheme. The current icing condition display shall be served on the Internet and be accessible to the FAA, and other interested parties, through a standard Web browser, in near real-time. Displays will be updated every 60 seconds and will have a maximum delay of no more than three minutes.

2.4.14. Covariance data shall be sent over the Internet and archived remotely. Because of the possibility of Internet outages, data shall be buffered locally until it has been sent. Sufficient local storage shall be provided to buffer data for 48 hours without loss of data.

2.4.15. The system shall monitor itself and send e-mail messages if a possible failure condition occurs. As much diagnostic information as practical shall be gathered and sent.

2.4.16. RADS shall meet the requirements specified in Table 4.

Parameter	Min	Nominal	Max	Units	Comment
A/D converter, channels	2				two parallel channels
A/D sampling rate	5			MHz	
A/D bits	12			Bits	
A/D dynamic range	65			dB	(S/N + D)
A/D buffer memory		1024		Ksamples	swinging buffer
Pulse repetition period (PRP)	50		1000	μsecs	
Resolution of PRP			1	μsecs	
Range gate delay	2			μsecs	
Resolution of range gate delay			1	μsecs	
Range gate spacing	0.20	1.5		μsecs	
Resolution of range gate spacing			0.1	μsecs	
Number of range gates	4		72		may vary based on other parameters

Table 4. RADS performance specifications.

3. Options

3.1. Improved cloud particle information

3.1.1. Dual angle beam positioning antenna

This option would allow the radar to alternate between a low pointing angle to a vertically pointing configuration, using limit switches, in no longer than one minute. The azimuth will be unchanged. This feature would be controlled automatically. The two limits can be mechanically changed within the range 30 and 90 degrees. Vertical pointing (90 deg.) would be most useful with the spectral processing option: the velocity spectrum shape could be used to infer the types of particles present. The radiometer antenna would move with the radar antenna.

3.2. Improved sensitivity

3.2.1. Spectral processing

Spectral processing may slightly increase the sensitivity of the radar by 1 to 2 dB; and, in conjunction with vertical pointing, provide more information about cloud particle type and distribution, to improve the icing algorithm.

3.2.2. Dual receiver

A dual receiver would allow return from the co-polar and cross-polar signal to be acquired simultaneously rather than alternately. For a constant observation time, this would increase the sensitivity in each channel by 3 dB.

3.3. Spare subsystems

3.3.1. Since lead times for many components is quite long, purchase of spare subsystems such as transmitter, mixers, computer parts would improve the mean time of repairs.

4. Testing and demonstration

4.1. Testing

The radar shall pass the following tests before being deployed for demonstration:.

4.1.1. Basic radar function test.

Transmit power and signal sensitivity will be tested and evaluated.

4.1.2. Radar calibration test.

GRIDS will be operated close to another K_a-band radar. Echo strength from atmospheric targets will be compared.

4.1.3. Local data archiving test. (with scheduling)

Typical operating modes will be scheduled and the data will be recorded in the radar for a period of at least one week. The data taken and the operation of the radar will be monitored to insure that the radar has operated continuously with no manual intervention. This test may be run concurrently with 4.1.4 and 4.1.6.

4.1.4. Remote data archiving test. (with scheduling)

Typical operating modes will be scheduled and the data will be archived remotely for a period of at least two weeks. The data taken and the operation of the radar will be monitored to insure that the radar has operated continuously with no manual intervention. This test may be run concurrently with 4.1.3 and 4.1.6.

4.1.5. System health test.

All potential system health conditions, both warning and critical, will be induced or simulated and the system will be monitored to insure that it responds in an appropriate manner.

4.1.6. Remote operation test.

The system will be started and stopped and parameters and schedules will be changed from a remote site.

4.1.7. Power interruption test.

While operating from a schedule and collecting data, power to the system shall be interrupted and restored to insure that the system recovers and resumes its schedule. Various power interruption times will be used to insure that the system responds appropriately in all cases.

4.1.8. System reliability test.

The systems will be operated unattended in a scheduling mode for a period of at least four weeks to insure that it operates reliably.

4.2. Delivery, Setup and Demonstration

4.2.1. Local setup and demonstration

GRIDS will be first demonstrated near the facility where it is produced, observing whatever atmospheric targets are available. It is likely there will be no clouds with icing conditions to test the icing algorithms, other than indication of no hazard.

4.2.2. Final site setup and demonstration

The system will be demonstrated operationally for four continuous months at a site and time selected by FAA, after successful local setup and demonstration.

5. Typical Operating Modes and Sensitivity

The following table shows the independent radar parameters for typical operating modes. Note that the vertical mode and spectral processing are optional. Parameters below the double line are independent parameters that may be altered in software. Parameters below the triple line are dependent parameters. *A single receiver switching between co-polarized and cross-polarized channels on a pulse-to-pulse basis is assumed.* Note that the dwell time and vertical range resolution are held constant in the table.

mode	40 deg slant	40 deg slant	vertical	vertical
radar wavelength	8.6 mm	8.6 mm	8.6 mm	8.6 mm
antenna diameter	3.0 m	3.0 m	3.0 m	3.0 m
peak transmitted power	1000 watts	1000 watts	1000 watts	1000 watts
elevation angle	40.2 degrees	40.2 degrees	90 degrees	90 degrees
pulse repetition period	110 μsecs	110 μsecs	71 μsecs	71 μsecs
pulse width	1.55 μsecs	1.55 μsecs	1.00 μsecs	1.00 μsecs
number of time-domain averages	1	1	1	10
number of FFT points	64 points	256 points	256 points	256 points
number of spectrum averaged	4261/channel	1065/channel	1650/channel	1650/channel
range gate spacing	1.55 μsecs	1.55 μsecs	1.00 μsecs	1.00 μsecs
number of range gates	69	69	67	67
receiver bandwidth	0.645 MHz	0.645 MHz	1.0 MHz	1.0 MHz
unambiguous radar range	16.49 km	16.49 km	10.64 km	10.64 km
minimum height	68 m	68 m	105 m	105 m
maximum usable height	10.2 km	10.2 km	10.0 km	10.0 km
maximum unambiguous radial velocity	±9.77 m/s	±9.77 m/s	±15.14 m/s	±1.51 m/s
maximum unambiguous horizontal velocity	±12.80 m/s	±12.80 m/s	NA	NA
time available for one spectrum computation	102 μsecs	408 μsecs	271 μsecs	2713 μsecs
duty cycle	1.41%	1.41%	1.41%	1.41%
average power	14.1 watts	14.1 watts	14.1 watts	14.1 watts
range resolution	232.3 meters	232.3 meters	150 meters	150 meters
height resolution	150.0 meters	150.0 meters	150 meters	150 meters
radial velocity resolution	0.305 m/s	0.076 m/s	0.118 m/s	0.012 m/s
dwell time	60 secs	60 secs	60 secs	60 secs
Estimated sensitivity at 5 km AGL using spectral processing	-64.9 dBZe	-61.9 dBZe	-64.7 dBZe	-59.7 dBZe
Estimated sensitivity at 6 km AGL using spectral processing	-63.3 dBZe	-60.3 dBZe	-63.1 dBZe	-58.1 dBZe
Estimated sensitivity at 10 km AGL using spectral processing	-58.9 dBZe	-55.9 dBZe	-58.7 dBZe	-53.7 dBZe

APPENDIX C

GRIDS Block Diagram (Detailed)

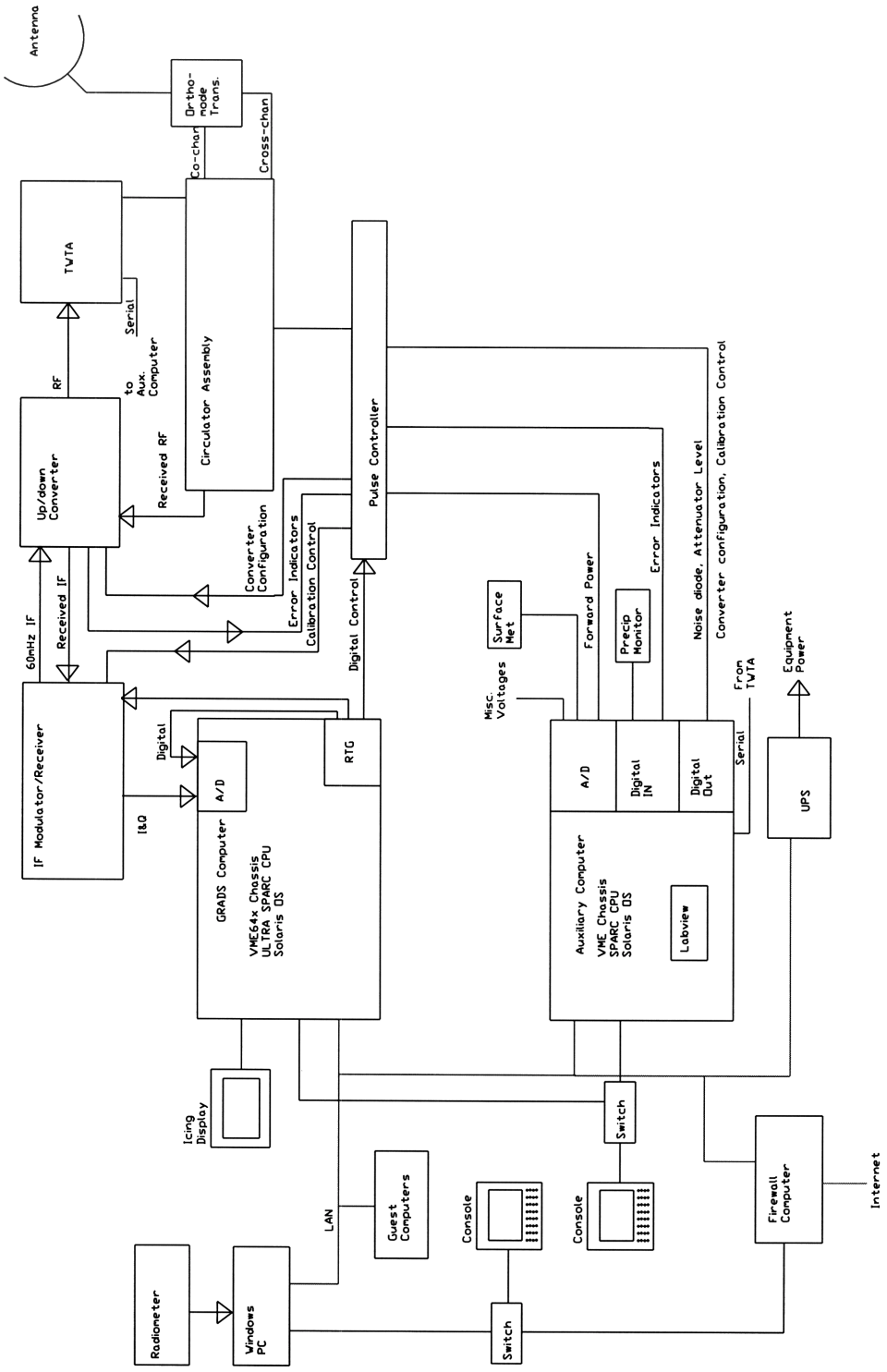

APPENDIX D

GRADS Data Flow Diagram

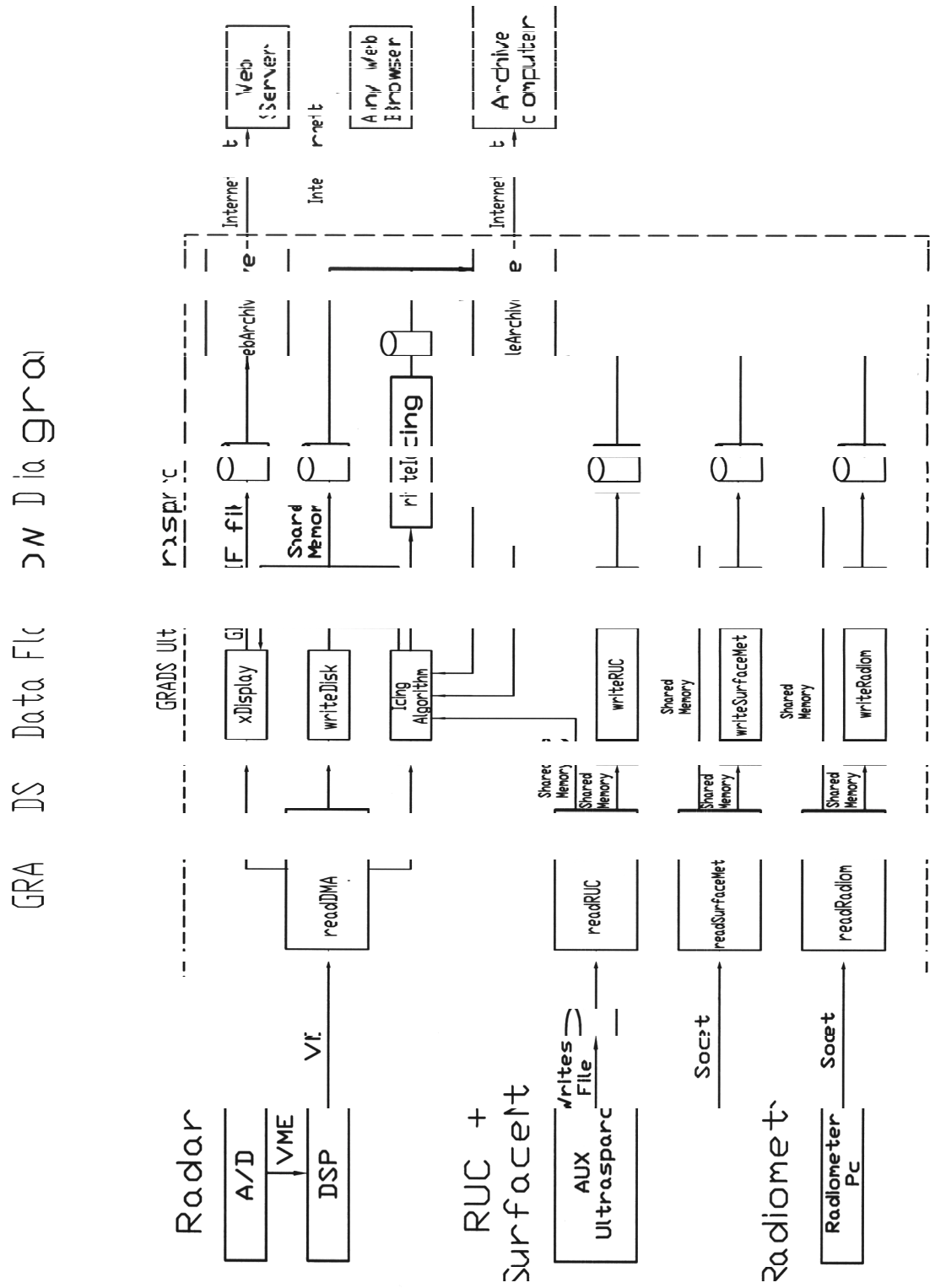

APPENDIX E

GRIDS Covariance Algorithms

Introduction

This document specifies the covariance-based algorithm that will be performed in real-time in GRIDS. This algorithm is commonly called the pulse-pair algorithm because it measures the phase difference between the received signal from a pair of radar pulses. With a very high signal-to-noise ratio, this phase difference and the time between the pulses is all that is required to calculate the Doppler shift and consequently the radial velocity of the target. In practice, the signals from many pairs of pulses are summed together to reduce the uncertainty of the estimate to an acceptable level.

Included is a brief introduction to covariances in the following section to give some context to the algorithm definitions.

Complex covariances and sine waves

The complex covariance function is used for many purposes in statistics, but here we use it only to calculate phase between two complex sine waves of the same frequency, and the power present in a complex wave. Complex quantities are in **bold** in the following equations.

The definition of complex covariance is given by

$$\mathbf{R}_{xy}(n) = \left\langle \left(\mathbf{X}_i^* - \left\langle \mathbf{X}^*{}_i \right\rangle\right) \bullet \left(\mathbf{Y}_{i+n} - \left\langle \mathbf{Y}_{i+n} \right\rangle\right) \right\rangle,$$

where $\mathbf{X_i}$ and $\mathbf{Y_i}$ represent complex time series and n represents the number of lags to use in calculating the covariance. The "< >" notation represents the average.

Simple algebra yields:

$$\mathbf{R}_{xy}(n) = \left\langle \mathbf{X}_i^* \mathbf{Y}_{i+n} \right\rangle - \left\langle \mathbf{X}_i^* \right\rangle \left\langle \mathbf{Y}_{i+n} \right\rangle = \mathbf{B}_{xy}(n) - \mathbf{A}_x^*(i)\mathbf{A}_y(i+n)$$

where $\mathbf{B_{xy}}(n)$, and $\mathbf{A}_x(n)$ and $\mathbf{A}_y(n)$ are defined for convenience. Note that $\mathbf{B_{xy}}(n)$ represents a "non-DC-corrected" version of the covariance, since $\mathbf{A}_x(n)$ and $\mathbf{A}_y(n)$ are the averages of a complex signal and are zero in the case of a signal with zero average.

Note that $\mathbf{R}_{xx}(0)$ is real-valued since

$$R_{xx}(0) = \left\langle \mathbf{X}_i^* \mathbf{X}_i \right\rangle - \left\langle \mathbf{X}_i^* \right\rangle \left\langle \mathbf{X}_i \right\rangle = \left\langle \left|\mathbf{X}_i\right|^2 \right\rangle - \left|\left\langle \mathbf{X}_i \right\rangle\right|^2$$

which represents the DC-corrected "power".

Now apply the covariance definition to two complex sine waves of the same frequency defined by

$$\mathbf{X} = Ae^{j\omega t}$$

$$\mathbf{Y} = Be^{j(\omega t+\varphi)}$$

where **Y** leads **X** by phase angle φ.

Then, since the expected value of a sine wave is zero,

$$\mathbf{R}_{xy}(0) = \left\langle \mathbf{X}_i^* \mathbf{Y}_i \right\rangle = \left\langle Ae^{-j\omega t} Be^{j(\omega t+\varphi)} \right\rangle = \left\langle ABe^{+j\varphi} \right\rangle = ABe^{+j\varphi}$$

and

$$\arg\left(\mathbf{R}_{xy}(0)\right) = \varphi .$$

This illustrates how the angle of the complex covariance function gives the phase difference between two sinusoidal signals of the same frequency. In the case of two consecutive pulses, this phase difference and the time between the pulses yields the Doppler shift. If we were calculating differential phase, this same property could be used to give the phase shift between the co- and cross-polarized signals.

Application of covariance functions to the GRIDS radar

The GRIDS radar will transmit a single circular polarization and receive sequentially on a pulse-to-pulse basis, a co-polarized signal and a cross-polarized signal. A future enhancement may allow the reception of both the co- and cross-polarized signals simultaneously. The nomenclature here will support either case; it does not, however, support any switching of transmit modes. We will adopt the convention of using a "c" to represent the signal received on the co-polarized channel, and an "x" to represent the signal received on the cross-polarized channel.

It is advantageous in the pulse-pair mode to receive two co-polarized pulses followed by two cross-polarized pulses. This doubles the maximum unambiguous velocity over what would be possible with a strictly alternating polarization. The radar will therefore operate in a double-pulse mode. Covariances of the form **R**(0), signifying zero lags, are formed from summing over every co- or cross-polarized *sample* in the beam, that is, both the first and second pulses of the pair. Covariances of the form **R**(1), signifying one lag, are formed from summing over every co- or cross-polarized *pair* in the beam, where the two factors in the covariance are taken from the first and second pulse of the pair.

The covariances we will use are shown in the table below. Complex quantities are in **bold**.

Symbol	**Description**	**Used to calculate:**
$R_{cc}(0)$	co-polarized "power"	co-polarized power
$R_{xx}(0)$	cross-polarized "power"	cross-polarized power
$\mathbf{R}_{cc}(1)$	co-polarized covariance, one lag	co-polarized pulse-pair velocity
$\mathbf{R}_{xx}(1)$	cross-polarized covariance, one lag	cross-polarized pulse-pair velocity

By calculating **B**'s and **A**'s separately in the DSP and passing those values to the SPARC, we make it possible to produce "non-DC-corrected" values of various quantities, such as received power, which may be useful for calibration. The table below shows "data products", which are quantities that are recorded. Total memory required is 56 bytes.

Calculated variable name	Mathematical symbol	Description	Required for
Ac0	$\mathbf{A}_c(0)$	average of co-polarized samples from first pulse of pair	DC correction
Ax0	$\mathbf{A}_x(0)$	average of cross-polarized samples from first pulse of pair	DC correction
Ac1	$\mathbf{A}_c(1)$	average of co-polarized samples from second pulse of pair	DC correction
Ax1	$\mathbf{A}_x(1)$	average of cross-polarized samples from second pulse of pair	DC correction
Bcc0	$B_{cc}(0)$	uncorrected co-polarized covariance, zero lag	power & pulse-pair width
Bxx0	$B_{xx}(0)$	uncorrected cross-polarized covariance, zero lag	power & pulse-pair width
Bcc1	$\mathbf{B}_{cc}(1)$	uncorrected co-polarized covariance, one lag	pulse-pair velocity & width
Bxx1	$\mathbf{B}_{xx}(1)$	uncorrected cross-polarized covariance, one lag	pulse-pair velocity & width

The following table shows the display (discarded) products. A "U" at the end of a name means that the value has been calculated from non-DC-corrected covariances. All of these quantities are calculated for each range gate.

Description	Derived from co-polarized channel	Derived from cross-polarized channel	Derived from both channels	Units
velocity	Vc	Vx		m/s
velocity spread	Wc	Wx		m^2/s^2
correlation	Cc	Cx		none
intensity (power at receiver output)	Ic, IcU	Ix, IxU		dBm
power (power at antenna terminals)	Pc, PcU	Px, PxU		dBm
Reflectivity factor	Zc, ZcU	Zx, ZxU		dBZ
circular depolarization ratio			CDR	dB

The following equations will be used to calculate DC-corrected covariances from the uncorrected covariances:

$$R_{cc}(0) = B_{cc}(0) - \frac{1}{2}\left[\left|\mathbf{A}_c(0)\right|^2 + \left|\mathbf{A}_c(1)\right|^2\right]$$

$$R_{xx}(0) = B_{xx}(0) - \frac{1}{2}\left[\left|\mathbf{A}_x(0)\right|^2 + \left|\mathbf{A}_x(1)\right|^2\right]$$

$$\mathbf{R}_{cc}(1) = \mathbf{B}_{cc}(1) - \mathbf{A}_c^*(0) \bullet \mathbf{A}_c(1)$$

$$\mathbf{R}_{xx}(1) = \mathbf{B}_{xx}(1) - \mathbf{A}_x^*(0) \bullet \mathbf{A}_x(1)$$

The following equations are shown with R's for the covariances, but will also be used with B's to calculate uncorrected quantities where required. In the following equations z_0 is the receiver impedance (50 ohms), rnh and rnv are the co-polarized and cross-polarized receiver gains, c_0 is the speed of light, k_{hRC} and k_{vRC} are the co- and cross-polarized radar constants, f_T is the transmit frequency, T_S is the time between the first and second pulses in the pair, R'(0) is covariance with receiver noise, and r is the range in meters.

$Vc = \frac{-c_0}{4\pi f_T T_S}\arg\left(\mathbf{R}_{cc}(1)\right)$	$Vx = \frac{-c_0}{4\pi f_T T_S}\arg\left(\mathbf{R}_{xx}(1)\right)$	m/s
$Wc = \frac{c_0^2}{8\pi^2 f_T^2 T_S^2}\left(1 - \frac{\left\|\mathbf{R}_{cc}(1)\right\|}{R_{cc}(0) - R'_{cc}(0)}\right)$	$Wx = \frac{c_0^2}{8\pi^2 f_T^2 T_S^2}\left(1 - \frac{\left\|\mathbf{R}_{xx}(1)\right\|}{R_{xx}(0) - R'_{xx}(0)}\right)$	m^2/s^2
$Cc = \frac{\left\|\mathbf{R}_{cc}(1)\right\|}{R_{cc}(0)}$	$Cx = \frac{\left\|\mathbf{R}_{xx}(1)\right\|}{R_{xx}(0)}$	none
$Ic = 10 \bullet \log\left(\frac{R_{cc}(0)}{z_0}\right) + 30$	$Ix = 10 \bullet \log\left(\frac{R_{xx}(0)}{z_0}\right) + 30$	dBm at rcvr output
$Pc = Ic - rnh$	$Px = Ix - rnv$	dBm at antenna
$Zc = Pc + k_{hRC} + 20 \bullet \log(r) - 60$	$Zx = Px + k_{vRC} + 20 \bullet \log(r) - 60$	dBZ
$CDR = Pc - Px$		dB

APPENDIX F

GRIDS IDDAS Software Capability Specifications

This document outlines the major software components that will be needed for the Icing Display and Data Acquisition System (IDDAS). It includes the eight major components for Upgradable GRIDS and eight additional components needed for Target GRIDS. Existing RADS (Radar Acquisition and Display System) and POP (Profiler On-line Program) software systems were studied; their desired features have been included in the IDDAS design.

I) IDDAS for Upgradable GRIDS

A) Data ingest

There will be four data streams, which will need to be ingested by IDDAS. These will be radar data, radiometer data, RUC data and surface meteorological data. There will be four different processes that ingest these data streams and communicate with the icing algorithm via shared memory objects. They come in at various times and are used in the icing algorithm, to determine hazardous conditions. These four data streams are described in detail below.

1) Radar data

IDDAS will interface to the DSP via global memory on the DSP board. A process called readDMA transfers the data in by a DMA operation. Covariance data (see **Appendix E**) will be ingested at this time, as defined in the *GRIDS Covariance Algorithms* document. The IDDAS design will allow for future additional modes such as spectra. These modes will be selectable by the user. The IDDAS will read and write Radar Parameters version 1.2 from shared memory, as outlined in the *RADS Radar Parameters Version 1.2* document.

Range gate limits will be operator enabled and 4 to 100 range gates will be available in this mode. The number of range gates in the usual operating mode will be 69. The maximum number of triggers will be 1,000,000, with a standard operating number of 779,221 triggers for a 60 second dwell. Typically the data rate will be one beam every 60 to 62.5 seconds.

As in the RADS design, readDma will ingest two different kinds of data; raw data and display data. It will send the display data to the process xDisplay (described in section C below) and will send the raw data to the disk for archival. Reflectivity and depolarization data will be sent to the icing algorithm process, icingAlg, described in section D below.

2) Radiometer data

Time stamped radiometer data will be sent to IDDAS from the Radiometer PC every minute via a TCP socket. Since the radiometer generates a point every 15-17 seconds, the software on the Radiometer PC will average the last four points, before sending them to the IDDAS process readRadiom every minute. The variables sent could be integrated liquid, integrated vapor, and brightness temperature from each channel. writeRadiom will append radiometer data into one hour files. These files are expected to be between 30-50 Kbytes per hour. Format and file naming conventions need to be defined. readRadiom will also send the data to the xDisplay process for display and the icingAlg process via shared memory. As stated in C.2 below, the radiometer displays will be updated as soon as IDDAS receives the data.

3) RUC data

RUC model output will be served to IDDAS from the AUX system approximately every hour. The timing will be driven by the update of RUC data on the Web. A file will appear via FTP on the GRADS machine. Format and filenames of these files will need to be defined, but must include the time and date. An IDDAS process readRUC will check for new RUC files on the hour and will send the necessary data to icingAlg and xDisplay via shared memory.

4) Surface meteorological data.

Every minute surface meteorological data will be served to IDDAS from the AUX system via a socket. This data includes temperature and humidity. A process called readSurf will listen for these packets and create a time stamped file every hour. The minute data will be appended into the hourly files. Format and filenames still need to be defined. ReadSurf will also send the minute data to the icingAlg process via shared memory.

B) Control Window Graphical user interface

There will be a graphical user interface (GUI) which controls the data ingest from all instruments and allows the operator to set various parameters. This process will be called the RCP. Some of the functions of the RCP will include turning on and off the various data streams, turning on and off the instruments and positioning the instruments. Below is the prototype GUI:

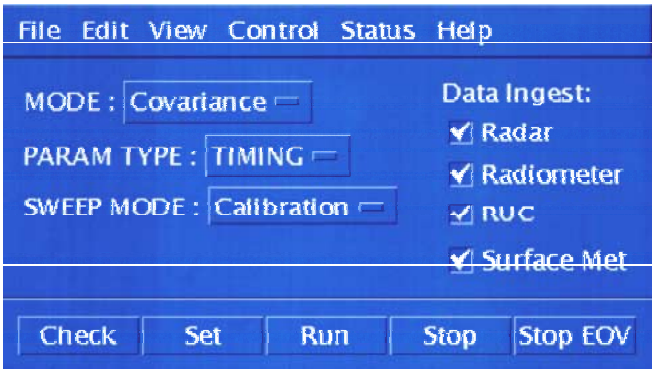

1) Data Ingest control

There are four data streams that need to be ingested by IDDAS in order to calculate the icing algorithm. These are from the radar, radiometer, surface meteorology, and RUC, as described in section A) above. The user will be able to turn these data streams on and off individually, but the icing algorithm is only calculated when all four of the data streams are turned on, which will be the default.

2) Data Archival

A separate archival function will be made available to the user. This switch will allow the user to turn on and off the archival capabilities. When the archival switch has been turned on (which will be the default) the four ingested data streams will be archived along with the generated icing GIF file and the results of the icing algorithm.

3) Instrument Control

The user will be able to run and pause the radar in continuous mode or in a queuing mode. The target system will include more extensive instrument control, including positioning, starting and stopping the radar and the radiometer. The user will be able to exit IDDAS from the GUI.

4) Radar Parameters

The user will be able to edit, store, load, list and check different individual control tables. They will also be able to show the names of the existing tables. These tables will allow users to indicate which mode they wish to run and to select which parameters to change (e.g., housekeeping) and display. An ID code has been added to the Radar Parameters (RDID) that the operator can change. The Radar Parameters do not include max duty cycle, max transmit pulse, and min ipp. We see no reason to put these limits in the Radar Parameters. The upgradable system will have only the covariance mode defined. The target

system may also have an additional mode for spectral processing.

The user will be able to create, edit, store, load, and list individual queues (lists of control parameters). This GUI allows the user to select 12 of the19 covariance data fields, to be sent to xDisplay for real-time graphics, to aid in diagnostic exercises.

C) Data Displays

When discussing displays, we must differentiate variables and fields. A variable is a function only of time (e.g., integrated liquid water). Variables like this are plotted as the y-coordinate versus time (x-coordinate). A field is a function of range and time, such as radar reflectivity. Here the magnitude of the field is indicated by a color on a plot of range (y-coordinate) vs. time (x-coordinate).

There is a separate IDDAS process called xDisplay that ingests data for display and displays them to the real-time screen. It has a GUI that allows the user to select display type (i.e., BSCAN, A_SCOPE, RADIOMETER, ICING) and field. It also allows the user to change the scale and range. It has both an erase and a GIF capture capability.

There will be four kinds of display types available for selection: Marching Range-time (formerly called BSCAN), range-time (A_SCOPE, including RUC model output), Marching Icing Displays (see iii below) and Marching Radiometer (see iv below). There will be no exit button from xDisplay.

Any field variable can be displayed on either the A-scope or Marching Range-Time display. These four types can be displayed simultaneously, but there can only be one of each type. Although the Icing Display has the same appearance as the Marching Range-Time display, it is different because it is displayed on the dedicated console, and because it can be displayed simultaneously with another Marching Range-Time display that shows an arbitrary field.

1) Radar Data Displays

For radar data, twelve of the nineteen possible fields (see **Appendix E**, GRIDS Covariance Algorithms) will be available one at a time for the Marching Range-time and A_scope displays. There will also be an additional button for Icing Displays and one or more buttons for Radiometer fields (see ii below).

Scaling may be changed for all twelve radar fields as well as the radiometer variables. Marching Range-time displays present a maximum of 600 beams or ten hours of radar data. A_Scope displays will be linear and not normalized as seen in current RADS. The user can change the scale of x for spectra and A_scopes and max range (or y) in time-height displays and A_scope displays.

2) Radiometer Data Displays

Radiometer data will be a display type. Plots will be x-y displays of integrated liquid water, integrated water vapor and two brightness temperatures vs. ten hours of time (on the x axis). The four variables will be plotted in different colors on the same display. This display type will operate like the other display types in that the user will be allowed to select the four radiometer variables from the field button list and then select corresponding scales and ranges for those variables. These plots will be updated every minute, as new radiometer data is ingested.

3) Icing Display

This is a marching range-time display that is updated every minute. It will also display ten hours of data. One local copy will be served on the console and one to another dedicated monitor. Changing the scale of the icing field will not affect the copy on the dedicated monitor. A GIF file of the current icing display on the dedicated monitor will be sent to Boulder every minute to be served over the Web no longer than three minutes behind real-time.

4) RUC Model Display

This is temperature vs. height. It will be shown in the A_scope window as a marching range-time display. It will be an additional field button, but not a separate display type. The user will be able to change the color scale for this field. The displays will be updated every minute even though the data is updated only once per hour or whenever new RUC data is ingested by the AUX system.

D) Perform the icing algorithm every minute and update the icing displays

A separate process in the IDDAS system called icingAlg, will perform the icing algorithm every minute using the most recent data from the RUC mode, the radar, the radiometer and surface meteorological input. The icing displays will be updated as described in C.3) above. The icing algorithm is performed on every beam of radar data, at every range gate. It uses reflectivity and depolarization data from the radar. See Reinking, et al. (2001) for further details.

E) Automatically capture the icing displays

Every minute the most recent icing display will be automatically captured as a GIF image and sent to a Web server in Boulder that will make them available on the Web. These will be updated every minute, not to be more than three minutes behind real-time.

F) Write data to disk

IDDAS will store raw radar data in EF (Extended UF) disk files. The SWTM parameter determines the size and length of time of the radar file. Covariance radar

files require 56 bytes per range gate. With 69 gates and 60-second beams, the files will be 291,840 bytes/hour (with a 1000-byte header on each beam). All file names will conform to a standard (yet to be determined) that will indicate type, location (radar parameter RDID) and time.

IDDAS will also store radiometer data, icing model output, GIF files of icing images, RUC files, and surface meteorological data as separate files. Formats and filenames have not yet been defined for these files. A problem with all of these files arriving asynchronously is determining which files were used in a particular icing model calculation. Therefore the icing model output should incorporate the file names (which will indicate time) that it used in its calculations.

IDDAS will save radiometer data to a separate file. It will append a data record onto this file every minute. At the end of the hour the file will be closed and sent to the archival system. The data rate generation for these files is expected to be 30-50 Kbytes per hour.

Surface meteorological data will be handled in the same way as radiometer data. Data will be ingested via a socket every minute and appended to an hourly file.

A new GIF file of the icing display is generated every minute and is sent to the Web server at that time. Once an hour the GIF file for the previous hour and half-hour will be sent to the archival system. These files are about 110 Kbytes each.

IDDAS will store the data for up to 48 hours, in case the archival link is unavailable.

G) Archive the data

There will be another process or script that SCPs the icing, radar, radiometer, RUC, GIF images and surface meteorological data to the archival system once an hour, unless the link is down. Once the files have been archived, they will be moved to another part of the disk for playback purposes.

Although a GIF file of the icing display will be sent to the server every minute, only two of the GIF files will be archived each hour; one for the hour and one for the half-hour.

H) Monitor disk usage and take appropriate action

Since it appears that a month's worth of data will take less than a gigabyte of storage space, the disk scrubbing process will only delete files after they are at least four weeks old.

II) IDDAS for Target GRIDS

A) Playback capabilities

Playback must be able to read from local data files that were previously archived. It will display the data, much as it does in real-time. Since it does not need to be a VME system or even have a DSP it can run on the AUX system or another SPARC system as well as the GRADS system. The icing images, radiometer displays, RUC display, surface plus the nineteen radar display fields need to be made available in playback mode. Therefore the archived RUC data, radar data, radiometer data, surface meteorological data and icing model data will need to be ingested by the playback machine.

B) On-line help

On-line help in the form of an on-line manual will be available.

C) React to system health messages

This includes power failure recovery and the ability to resume scheduled activities without operator intervention. Items to be discussed include how often health messages should be sent and in what format. Trouble messages would come over from AUX machine with an error code. A tabular structure might be used to categorize responses for each trouble. For every kind of trouble there might be several possible actions that can be defined (note that several actions could be selected for each problem although some are mutually exclusive), including ignore, print message on console, e-mail message, stop and restart, permanently stop, execute a special routine and continue, execute a special routine and restart, *etc*.

D) Allow remote monitoring

GRADS will run autonomously and remote monitoring will be available via a web interface.

E) Receiver calibration verification at scheduled intervals

See section 4.4 for a further discussion of receiver calibration.

F) Spectral processing and displays

This mode has not been defined yet and will have its own associated parameters, including windowing, number of spectral points, spectral averaging, and dc filtering. For display purposes, it will be its own display type. The user will need to be able to change the color scale, but may not be able to change ranges.

G) Radar/radiometer control

This will include pause/start, position and shutdown. The AUX system will do the actual shutdown of the radar, which can be initiated by either UPS software or by IDDAS. Computers' shutdown shall be independent of power disconnect to the instruments.

H) Enhanced Icing Hazard Algorithm

See section 4.3.2 for a further discussion of the enhanced icing hazard algorithm.

APPENDIX G

Enhancements to Core Icing Algorithm For Target GRIDS

LW Enhancement. The value of the path-integrated LW sensed by the microwave radiometer can be distributed throughout those cloud layers that have liquid water, to estimate LWC (g m^{-3}) in each liquid layer and hence the potential severity of the icing hazard. LW of 1 mm equates to an average LWC of 1 g m^{-3} in a cloud 1 km deep. In FAR Appendix C, the minimum LWC threshold for moderate icing is at the point (LWC, D_e, T) = (0.06 g m^{-3}, 40 μm, 20º C).

Here is an outline of how it will work in Upgradable GRIDS:

We assign liquid only to clouds for which Z_e > -23 dBZ, and assume that any part of a cloud with a lower reflectivity has minimal LWC.

(a) If *Condition Red* is met over the entire cloud path: Determine this path length from radar measurements and normalize liquid water path (LWP) to it. If LWC < 0.06 g m^{-3}, the potential icing hazard is minimal. If 0.06 g m^{-3} > LWC > 0.1 g m^{-3} light to moderate icing is possible. If LWC > 0.1 g m^{-3}, severe icing is possible. These "break point" values are the most conservative (smallest) within FAR Appendix C envelopes. Experience with GRIDS may show that the break point values should be adjusted.

(b) If *Condition Red* is met over only part of the cloud where Z_e > -23 dBZ, and the rest of the cloud is *Condition Yellow* or warm *(Condition Green)*, two options are available:

> (1) Allocate all liquid to that depth of the cloud where *Condition Red* is met. This is the most conservative approach, yielding maximum value of LWC and likely overestimating the potential icing severity. This approach excludes allocating any liquid to additional parts of clouds that may be mixed phase (*Condition Yellow)* or to any warm cloud (*Condition Green*).
>
> (2) Assign equal LWC to liquid (or potentially liquid) cloud paths of all three conditions. This is the less conservative approach that may underestimate the potential icing hazard.

(c) If *Condition Yellow* is met and there is no cloud along the path rated *Condition Red*: Assign LWC by either of the two options in (b) above.

The table below classifies potential icing hazard according to LWC. A Condition Red carries more weight than a Condition Yellow with the same LWC, because the ice particles in the Condition Yellow will tend to consume the liquid by vapor deposition or riming.

Condition	**LWC** ($g\ m^{-3}$)	**Hazard Rating**
Red	$LWC \geq 0.1$	Red-1
	$0.06 \leq LWC < 0.1$	Red-2
	$LWC < 0.06$	Red-3
Yellow	$LWC \geq 0.1$	Yellow-1
	$0.06 \leq LWC < 0.1$	Yellow-2
	$LWC < 0.06$	Yellow-3
Green	LWC (any value)	Green

T Enhancement. Further refinement of the potential icing hazard is possible via temperature classification. A statistical study (Schultz and Politovich, 1992) estimated that approximately 90% of icing incidents occur in the temperature range of 0º C to -20 º C, and 70% occur when -15º C < T < -2º C. Icing potential increases with temperature because warmer air can hold more vapor and thus produce more condensed liquid. A temperature classification such that T ≤ 20º C means minimal risk, -20º C < T ≤ -10º C means moderate risk, -10º C < T < 0º C means highest risk, and T > 0º C means no risk could be applied alone, or in combination with the LWC stratification. Since temperature and LWC are not truly independent, applying an additional temperature classification becomes somewhat redundant and adds complication. Still, from each point (LWC, T) in the cloud profile, it may be possible to estimate not only the icing severity, but also the *droplet size (D_e)* that is contributing to the hazard. After a sufficient set of GRIDS data are acquired and analyzed, it will be possible to study such enhancements.

Bright band (melting level) enhancement. Freezing drizzle and rain occur at the surface when falling snowflakes melt, and the droplets they create fall into colder, sub-cooled air nearer the surface. The first indicator is evidence of a bright band (the melting layer). It is lucidly depicted by the GRIDS radar as a line of extremely high depolarization (DR approaching 0 dB, the level for complete depolarization), clearly separated from much lower DRs immediately above and below the melting level. GRIDS will also show the minimal, signature value of DR in freezing drizzle, but may show a DR that decreases with range in freezing rain due to attenuation. However, the latter effect at the 40º antenna elevation will be much reduced from that measured at lower elevations commonly used with scanning radars. Also, a $Z_e > -15$ dBZ in all range gates between the surface and the bright band will show that this hazardous precipitation is reaching the surface. The GRIDS surface temperature and/or the ingested temperature profile will indicate if the necessary supercooling is occurring below the melting level. Algorithms for detecting freezing drizzle and rain by measuring the vertical DR gradient to isolate the

bright band have been developed for other applications and will be adapted to GRIDS.

Vertically-pointing enhancment (depolarization and vertical motion measurements). The *Target* GRIDS radar is designed with options to replace pulse-pair processing with spectral processing, and to add a zenith-pointing capability. Transmissions to zenith and the 40º elevation in alternating 5 min periods would provide superior ice particle identification in DR, as well as measurements of Doppler vertical velocity and vertical velocity variance. The pointing angle of microwave radiometer would alternate in sychronization with that of the radar. Spectral processing could add sensitivity to the radar, and if implemented with the zenith-pointing option, would provide spectral measurements of the vertical velocity. Formulations of specific algorithm enhancements from these additional measurements offer considerable promise.

The identification of the different ice particles in itself can add another level of confidence to detection of an icing condition, especially in those clouds of mixed-phase. Ice crystal families can be identified and differentiated from droplets with a high level of confidence in 40º elevation DR measurement alone. However, the specific type of ice particle and changes in particle type are best established by measuring DR as a function of a full range of elevation angles, or at a minimum of two elevation angles including zenith. Ice types are indicators of the microphysical processes that are active in a cloud, and hence of the likely rate of consumption of hazardous liquid by ice. For example, the presence of pristine ice crystals indicates minimal riming of the crystals by cloud droplet collection, and thus a minimal icing hazard. However, the presence of graupel is normally indicative of liquid-producing convection; it shows that considerable liquid-consuming riming has occurred, and warns that liquid build-up may occur in successive convective elements.

Doppler velocity parameters can be used to estimate both vertical air motion and the falling speed of hydrometors when the radar is pointed to zenith. Mixed-phase clouds can produce droplets of sufficient size and LWC to be an icing hazard only if upward air motion is sufficient to condense liquid faster than the ice can consume it. Strong upward air motion can be liquid-producing when it exceeds the terminal velocity of ice particles (hail excluded). Vertical velocity spectra might help decide if the cloud is of single or mixed phase, and they can be used to estimate the *effective size* of any droplets from *differences* in ice particle and cloud droplet fallspeed (Zawadski et al. 2000).

The addition of zenith pointing measurements of DR and the vertical velocity parameters are expected to provide significant additional value to the GRIDS measurements, not only by enhancing the estimate of the potential icing hazard in mixed phase clouds, but also by indicating the vertical atmospheric forcing and turbulence that produces those conditions.

APPENDIX H
Upgradable GRIDS Gantt Chart

(if missing, please view accompanying .pdf file)

APPENDIX I

Table of GRIDS Features and Benefits

Feature	Benefit	Implemented on	Comment
TWTA (traveling wave tube amplifier) transmitter	Longer lifetime than magnetron tube. Allows for higher transmit power, if necessary.	Upgradable	Borrowed component on upgradable system. Higher power would require a longer pulse, which means pulse coding would have to be implemented.
MMCR-based radar design	Mature design that has performed well in the several deployed MMCRs.	Upgradable	Borrowed components on upgradable system.
RADS-based computer design	RADS was developed by current staff and has performed well in ETL's research radars. Allows for complete visibility of all data in real time.	Upgradable	
Critical computers are VME based.	Provides a design with a long lifetime despite rapid advances in computer technology. CPU advances can be easily incorporated. Chassis allows for additional interface boards.	Upgradable	Twenty-year old industrial-grade bus design has always maintained backward compatibility, even though its performance has been enhanced several times to give it state-of-the-art performance.
Housed in seatainer	Allows for easy, inexpensive shipping. Inexpensive, rugged container. Strong enough to serve as a mounting point for the antenna.	Upgradable	Works especially well for transport by ship or barge.
Icing data served by remote server	Allows for many simultaneous accesses to icing data without compromising the performance of GRIDS.	Upgradable	
Data archived remotely	Eliminates the need for local operators.	Upgradable	

"Mailbox" radiometer	Commercially available radiometer is easy to procure.	Upgradable	Borrowed component on upgradable system.
System UPS	Protects system from intermittent power outages. Allows for complete unattended recovery from a power outage.	Target	The UPS will be available on the upgradable system, but a complete recovery from a power interruption will only be implemented on the target system.
Monitoring and notification of system health	Allows the system to work without constant attention of a technician.	Target	Some monitoring will be done on upgradable system, but full implementation will wait for the target.
Firewall computer	Protects other computers from computer vandals. Simplifies computer security.	Upgradable	Most security updates need only be implemented on the firewall computer. This enhances the stability of the other computer systems.
Spectral processing	Improves performance in conditions of low signal.	Target	Covariance processing will be available on the upgradable.
Moveable antenna (slant and vertical operation)	In conjunction with spectral processing, differentiates ice vs. droplet fall velocities to enhance icing algorithm in mixed phase clouds.	Option	
Dual receiver	Improves performance in conditions of low signal by 3 dB.	Option	
Spares	Improves mean time to repair, dramatically so in the case of a failure of a radar component	Option	Some radar components have delivery times of many months.
Complete system	Designed to be close to an operational prototype. Would allow systems to be put into production quickly.	Target	